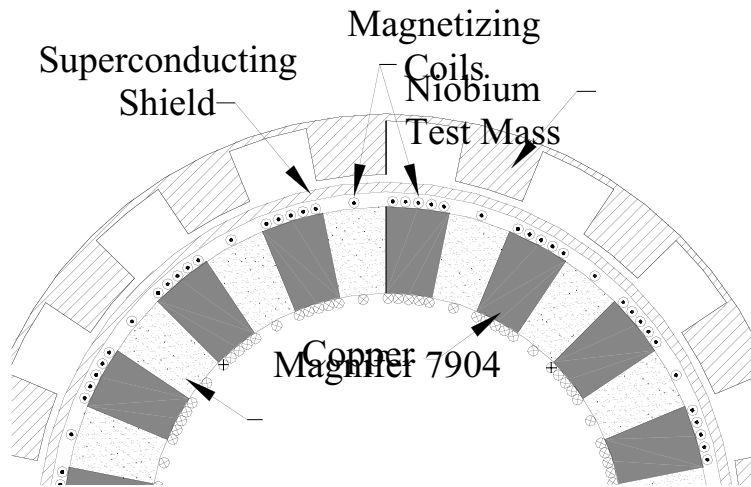
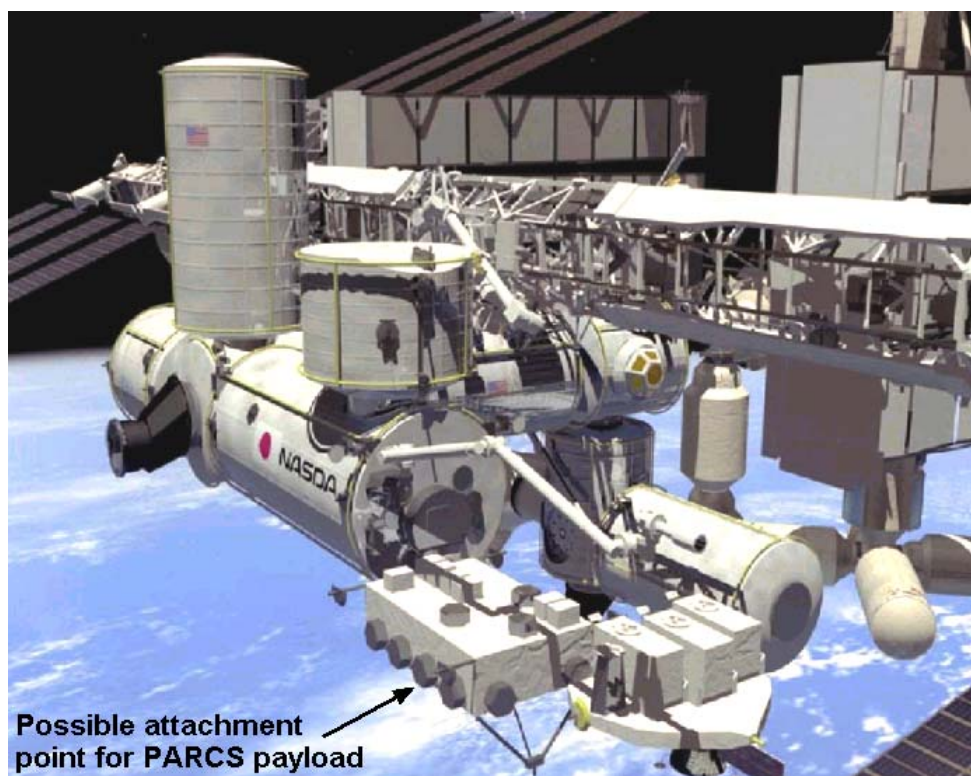


CHAPTER 4

GRAVITATION AND RELATIVITY PHYSICS





GRAVITY AS A KEY PROBLEM OF THE MILLENIUM

Vitaly N. Melnikov

*Institute of Gravitation and Cosmology, Peoples' Friendship University of Russia, 6 Miklukho-Maklaya St., Moscow 117198, and
Center for Gravitation and Fundamental Metrology, VNIIMS, 3-1 M. Ulyanovoy St., Moscow 117313, Russia
and Depto.de Fisica, CINVESTAV, Apartado Postal 14-740, Mexico 07360, D.F.¹*

Gravitation as a fundamental interaction that governs all phenomena at large and very small scales, but still not well understood at a quantum level, is a missing cardinal link to unification of all physical interactions. Problems of the absolute G measurements and its possible time and range variations are reflections of the unification problem. Integrable multidimensional models of gravitation and cosmology make up one of the proper approaches to study basic issues and strong field objects, the Early Universe and black hole physics in particular. The choice, nature, classification and precision of determination of fundamental physical constants are described. The problem of their temporal variations is also discussed, temporal and range variations of G in particular. A need for further absolute measurements of G , its possible range and time variations is pointed out. The novel multipurpose space project SEE, aimed for measuring G and its stability in space and time 3-4 orders better than at present, may answer many important questions posed by gravitation, cosmology and unified theories.

1. Introduction

The second half of the 20th century in the field of gravitation was devoted mainly to theoretical study and experimental verification of general relativity and alternative theories of gravitation with a strong stress on relations between macro and microworld phenomena or, in other words, between classical gravitation and quantum physics. Very intensive investigations in these fields were done in Russia by M.A.Markov, K.P.Staniukovich, Ya.B.Zeldovich, A.D.Sakharov and their colleagues starting from mid 60's. As a motivation there were: singularities in cosmology and black hole physics, role of gravity at large and very small (planckian) scales, attempts to create a quantum theory of gravity as for other physical fields, problem of possible variations of fundamental physical constants etc. A lot of work was done along such topics as [3]: - particle-like solutions with a gravitational field, - quantum theory of fields in a classical gravitational background, - quantum cosmology with fields like a scalar one, - self-consistent treatment of quantum effects in cosmology, - development of alternative theories of gravitation: scalar-tensor, gauge, with torsion, bimetric etc. As all attempts to quantize general relativity in a usual manner failed and it was proved that it is not renormalizable, it became clear that the promising trend is along the lines of unification of all physical interactions which started in the 70's. About this time the experimental investigation of gravity in strong fields and gravitational waves started giving a powerful speed up in theoretical studies of such objects as pulsars, black holes, QSO's, AGN's, Early Universe etc., which continues now. But nowadays, when we think about the most important lines of future developments in physics, we may foresee that gravity will be essential not only by itself, but as a missing cardinal link of some theory, unifying all existing physical interactions: weak, strong and electromagnetic ones. Even in experimental activities some crucial next

¹e-mail: melnikov@rgs.phys.msu.su, melnikov@fis.cinvestav.mx

generation experiments verifying predictions of unified schemes will be important. Among them are: STEP - testing the corner stone Equivalence Principle, SEE - testing the inverse square law (or new nonnewtonian interactions), EP, possible variations of the newtonian constant G with time, absolute value of G with unprecedented accuracy [39]. Of course, gravitational waves problem, verification of torsional, rotational (GPB), 2nd order and strong field effects remain important also. We may predict as well that thorough study of gravity itself and within the unified models will give in the next century and millenium even more applications for our everyday life as electromagnetic theory gave us in the 20th century after very abstract fundamental investigations of Faraday, Maxwell, Poincare, Einstein and others, which never dreamed about such enormous applications of their works. Other very important feature, which may be envisaged, is an increasing role of fundamental physics studies, gravitation, cosmology and astrophysics in particular, in space experiments. Unique microgravity environments and modern technology outbreak give nearly ideal place for gravitational experiments which suffer a lot on Earth from its relatively strong gravitational field and gravitational fields of nearby objects due to the fact that there is no ways of screening gravity. In the developement of relativistic gravitation and dynamical cosmology after A. Einstein and A. Friedmann, we may notice three distinct stages: first, investigation of models with matter sources in the form of a perfect fluid, as was originally done by Einstein and Friedmann. Second, studies of models with sources as different physical fields, starting from electromagnetic and scalar ones, both in classical and quantum cases (see [3]). And third, which is really topical now, application of ideas and results of unified models for treating fundamental problems of cosmology and black hole physics, especially in high energy regimes. Multidimensional gravitational models play an essential role in the latter approach. The necessity of studying multidimensional models of gravitation and cosmology [1, 2] is motivated by several reasons. First, the main trend of modern physics is the unification of all known fundamental physical interactions: electromagnetic, weak, strong and gravitational ones. During the recent decades there has been a significant progress in unifying weak and electromagnetic interactions, some more modest achievements in GUT, supersymmetric, string and superstring theories. Now, theories with membranes, p -branes and more vague M- and F-theories are being created and studied. Having no definite successful theory of unification now, it is desirable to study the common features of these theories and their applications to solving basic problems of modern gravity and cosmology. Moreover, if we really believe in unified theories, the early stages of the Universe evolution and black hole physics, as unique superhigh energy regions, are the most proper and natural arena for them. Second, multidimensional gravitational models, as well as scalar-tensor theories of gravity, are theoretical frameworks for describing possible temporal and range variations of fundamental physical constants [3, 4, 5, 6]. These ideas have originated from the earlier papers of E. Milne (1935) and P. Dirac (1937) on relations between the phenomena of micro- and macro-worlds, and up till now they are under thorough study both theoretically and experimentally. Lastly, applying multidimensional gravitational models to basic problems of modern cosmology and black hole physics, we hope to find answers to such long-standing problems as singular or nonsingular initial states, creation of the Universe, creation of matter and its entropy, acceleration, cosmological constant, origin of inflation and specific scalar fields which may be necessary for its realization, isotropization and graceful exit problems, stability and nature of fundamental constants [4], possible number of extra dimensions, their stable compactification etc. Bearing in mind that multidimensional gravitational models are certain generalizations of general relativity which is tested reliably for weak fields up to 0.001 and partially in strong fields (binary pulsars), it is quite natural to inquire about their possible observational or experimental windows. From what we already know, among these windows are: – possible deviations from the

Newton and Coulomb laws, or new interactions, – possible variations of the effective gravitational constant with a time rate smaller than the Hubble one, – possible existence of monopole modes in gravitational waves, – different behaviour of strong field objects, such as multidimensional black holes, wormholes and p -branes, – standard cosmological tests etc. Since modern cosmology has already become a unique laboratory for testing standard unified models of physical interactions at energies that are far beyond the level of the existing and future man-made accelerators and other installations on Earth, there exists a possibility of using cosmological and astrophysical data for discriminating between future unified schemes. As no accepted unified model exists, in our approach we adopt simple, but general from the point of view of number of dimensions, models based on multidimensional Einstein equations with or without sources of different nature: – cosmological constant, – perfect and viscous fluids, – scalar and electromagnetic fields, – their possible interactions, – dilaton and moduli fields, – fields of antisymmetric forms (related to p -branes) etc. Our program's main objective was and is to obtain exact self-consistent solutions (integrable models) for these models and then to analyze them in cosmological, spherically and axially symmetric cases. In our view this is a natural and most reliable way to study highly non-linear systems. It is done mainly within Riemannian geometry. Some simple models in integrable Weyl geometry and with torsion were studied as well. Here we dwell mainly upon some problems of fundamental physical constants, the gravitational constant in particular, upon the SEE project shortly (see A.Sanders' paper in this volume) and exact solutions in the spherically symmetric case, black hole and PPN parameters for these solutions in particular, within a multidimensional gravity.

2. Fundamental physical constants

2.1. In any physical theory we meet constants which characterize the stability properties of different types of matter: of objects, processes, classes of processes and so on. These constants are important because they arise independently in different situations and have the same value, at any rate within accuracies we have gained nowadays. That is why they are called fundamental physical constants (FPC) [3]. It is impossible to define strictly this notion. It is because the constants, mainly dimensional, are present in definite physical theories. In the process of scientific progress some theories are replaced by more general ones with their own constants, some relations between old and new constants arise. So, we may talk not about an absolute choice of FPC, but only about a choice corresponding to the present state of the physical sciences. Really, before the creation of the electroweak interaction theory and some Grand Unification Models, it was considered that this *choice* is as follows:

$$c, \hbar, \alpha, G_F, g_s, m_p \text{ (or } m_e), G, H, \rho, \Lambda, k, I, \quad (1)$$

where α , G_F , g_s and G are constants of electromagnetic, weak, strong and gravitational interactions, H , ρ and Λ are cosmological parameters (the Hubble constant, mean density of the Universe and cosmological constant), k and I are the Boltzmann constant and the mechanical equivalent of heat which play the role of conversion factors between temperature on the one hand, energy and mechanical units on the other. After adoption in 1983 of a new definition of the meter ($\lambda = ct$ or $\ell = ct$) this role is partially played also by the speed of light c . It is now also a conversion factor between units of time (frequency) and length, it is defined with the absolute (null) accuracy. Now, when the theory of electroweak interactions has a firm experimental basis

and we have some good models of strong interactions, a more preferable choice is as follows:

$$\hbar, (c), e, m_e, \theta_w, G_F, \theta_c, \Lambda_{QCD}, G, H, \rho, \Lambda, k, I \quad (2)$$

and, possibly, three angles of Kobayashi-Maskawa — θ_2 , θ_3 and δ . Here θ_w is the Weinberg angle, θ_c is the Cabibbo angle and Λ_{QCD} is a cut-off parameter of quantum chromodynamics. Of course, if a theory of four known now interactions will be created (M-, F-or other), then we will probably have another choice. As we see, the macro constants remain the same, though in some unified models, i.e. in multidimensional ones, they may be related in some manner (see below). From the point of view of these unified models the above mentioned ones are low energy constants. All these constants are known with different *accuracies*. The most precisely defined constant was and remain the speed of light c : its accuracy was 10^{-10} and now it is defined with the null accuracy. Atomic constants, e , \hbar , m and others are determined with errors $10^{-6} \div 10^{-8}$, G up to 10^{-4} or even worse, θ_w — up to 10%; the accuracy of H is also about 10%. An even worse situation is now with other cosmological parameters (FPC): mean density estimations vary within an order of magnitude; for Λ we have now data that its corresponding density exceeds the matter density (0.7 of the total mass). As to the *nature* of the FPC, we may mention several approaches. One of the first hypotheses belongs to J.A. Wheeler: in each cycle of the Universe evolution the FPC arise anew along with physical laws which govern this evolution. Thus, the nature of the FPC and physical laws are connected with the origin and evolution of our Universe. A less global approach to the nature of dimensional constants suggests that they are needed to make physical relations dimensionless or they are measures of asymptotic states. Really, the speed of light appears in relativistic theories in factors like v/c , at the same time velocities of usual bodies are smaller than c , so it plays also the role of an asymptotic limit. The same sense have some other FPC: \hbar is the minimal quantum of action, e is the minimal observable charge (if we do not take into account quarks which are not observable in a free state) etc. Finally, FPC or their combinations may be considered as natural scales determining the basic units. While the earlier basic units were chosen more or less arbitrarily, i.e., the second, meter and kilogram, now the first two are based on stable (quantum) phenomena. Their stability is believed to be ensured by the physical laws which include FPC. Another interesting problem, which is under discussion, is why the FPC have values in a very narrow range necessary for supporting life (stability of atoms, stars lifetime etc.). There exist several possible but far from being convincing explanations [40]. First, that it is a good luck, no matter how improbable is the set of FPC. Second, that life may exist in other forms and for another FPC set, of which we do not know. Third, that all possibilities for FPC sets exist in some universe. And the last but not the least: that there is some cosmic fine tuning of FPC: some unknown physical processes bringing FPC to their present values in a long-time evolution, cycles etc. An exact knowledge of FPC and precision measurements are necessary for testing main physical theories, extension of our knowledge of nature and, in the long run, for practical applications of fundamental theories. Within this, such theoretical problems arise: 1) development of models for confrontation of theory with experiment in critical situations (i.e. for verification of GR, QED, QCD, GUT or other unified models); 2) setting limits for spacial and temporal variations of FPC. As to a *classification* of FPC, we may set them now into four groups according to their generality: 1) Universal constants such as \hbar , which divides all phenomena into quantum and nonquantum ones (micro- and macro-worlds) and to a certain extent c , which divides all motions into relativistic and non-relativistic ones; 2) constants of interactions like α , θ_w , Λ_{QCD} and G ; 3) constants of elementary constituencies of matter like m_e , m_w , m_x , etc., and 4) transformation multipliers such as k , I and partially c . Of course, this division into classes is not absolute. Many constants move from one class to another. For example, e was a charge of

a particular object – electron, class 3, then it became a characteristic of class 2 (electromagnetic interaction, $\alpha = \frac{e^2}{\hbar c}$ in combination with \hbar and c); the speed of light c has been in nearly all classes: from 3 it moved into 1, then also into 4. Some of the constants ceased to be fundamental (i.e. densities, magnetic moments, etc.) as they are calculated via other FPC. As to the *number* of FPC, there are two opposite tendencies: the number of “old” FPC is usually diminishing when a new, more general theory is created, but at the same time new fields of science arise, new processes are discovered in which new constants appear. So, in the long run we may come to some minimal choice which is characterized by one or several FPC, maybe connected with the so-called Planck parameters — combinations of c , \hbar and G :

$$\begin{aligned} L &= \left(\frac{\hbar G}{c^3} \right)^{1/2} \sim 10^{-33} \text{ cm}, \\ m_L &= (c\hbar/2G)^{1/2} \sim 10^{-5} \text{ g}, \\ \tau_L &= L/c \sim 10^{-43} \text{ s}. \end{aligned} \quad (3)$$

The role of these parameters is important since m_L characterizes the energy of unification of four known fundamental interactions: strong, weak, electromagnetic and gravitational ones, and L is a scale where the classical notions of space-time loose their meaning.

2.2. The problem of the gravitational constant G measurement and its stability is a part of a rapidly developing field, called gravitational-relativistic metrology (GRM). It has appeared due to the growth of measurement technology precision, spread of measurements over large scales and a tendency to the unification of fundamental physical interaction [6], where main problems arise and are concentrated on the gravitational interaction. The main subjects of GRM are: - general relativistic models for different astronomical scales: Earth, Solar System, galaxies, cluster of galaxies, cosmology - for time transfer, VLBI, space dynamics, relativistic astrometry etc. (pioneering works were done in Russia by Arifov and Kadyev, Brumberg in 60's); - development of generalized gravitational theories and unified models for testing their effects in experiments; - fundamental physical constants, G in particular, and their stability in space and time; - fundamental cosmological parameters as fundamental constants: cosmological models studies, measurements and observations; - gravitational waves (detectors, sources...); - basic standards (clocks) and other modern precision devices (atomic and neutron interferometry, atomic force spectroscopy etc.) in fundamental gravitational experiments, especially in space... There are three problems related to G , which origin lies mainly in unified models predictions: 1) absolute G measurements, 2) possible time variations of G , 3) possible range variations of G – non-Newtonian, or new interactions.

Absolute measurements of G . There are many laboratory determinations of G with errors of the order 10^{-3} and only 4 on the level of 10^{-4} . They are (in $10^{-11} \text{ m}^3 \text{ kg}^{-1} \text{ s}^{-2}$):

1. Facy and Pontikis, France	1972 —	$6,6714 \pm 0.0006$	From this table it is evident that the
2. Sagitov et al., Russia	1979 —	$6,6745 \pm 0.0008$	
3. Luther and Towler, USA	1982 —	$6,6726 \pm 0.0005$	
4. Karagioz, Russia	1988 —	$6,6731 \pm 0.0004$	

first three experiments contradict each other (the results do not overlap within their accuracies). And only the fourth experiment is in accord with the third one. The official CODATA value of 1986

$$G = (6,67259 \pm 0.00085) \cdot 10^{-11} \cdot \text{m}^3 \cdot \text{kg}^{-1} \cdot \text{s}^{-2} \quad (4)$$

is based on the Luther and Towler determination. But after very precise measurements of G in Germany and New Zealand the situation became more vague. Their results deviate from

the official CODATA value by more than 600 ppm. As it may be seen from the Cavendish conference data [53], the results of 7 groups may agree with each other only on the level 10^{-3} . The most recent and precise G -measurement [56] diverge also from the CODATA value of 1986. This means that either the limit of terrestrial accuracies has been reached or we have some new physics entering the measurement procedure [6]. The first means that, maybe we should turn to space experiments to measure G [39], and second means that a more thorough study of theories generalizing Einstein's general relativity or unified theories is necessary. There exist also some satellite determinations of G (namely $G \cdot M_{\text{Earth}}$) on the level of 10^{-9} and several less precise geophysical determinations in mines. The precise knowledge of G is necessary, first of all, as it is a FPC; next, for the evaluation of mass of the Earth, of planets, their mean density and, finally, for construction of Earth models; for transition from mechanical to electromagnetic units and back; for evaluation of other constants through relations between them given by unified theories; for finding new possible types of interactions and geophysical effects; for some practical applications like increasing of modern gradiometers precision, as they demand a calibration by a gravitational field of a standard body depending on G : high accuracy of their calibration (10^{-5} - 10^{-6}) requires the same accuracy of G . (I am indebted to Dr.N.Kolosnitsyn for this last remark.) The knowledge of constants values has not only a fundamental meaning but also a metrological one. The modern system of standards is based mainly on stable physical phenomena. So, the stability of constants plays a crucial role. As all physical laws were established and tested during the last 2-3 centuries in experiments on the Earth and in the near space, i.e. at a rather short space and time intervals in comparison with the radius and age of the Universe, the possibility of slow *variations* of constants (i.e. with the rate of the evolution of the Universe or slower) cannot be excluded a priori. So, the assumption of absolute stability of constants is an extrapolation and each time we must test it.

2.3. Time Variations of G . The problem of variations of FPC arose with the attempts to explain the relations between micro- and macro-world phenomena. Dirac was the first to introduce (1937) the so-called "Large Numbers Hypothesis" which relates some known very big (or very small) numbers with the dimensionless age of the Universe $T \sim 10^{40}$ (age of the Universe in seconds 10^{17} , divided by the characteristic elementary particle time 10^{-23} seconds). He suggested (after Milne in 1935) that the ratio of the gravitational to strong interaction strengths, $Gm_p^2/\hbar c \sim 10^{-40}$, is inversely proportional to the age of the Universe: $Gm_p^2/\hbar c \sim T^{-1}$. Then, as the age varies, some constants or their combinations must vary as well. Atomic constants seemed to Dirac to be more stable, so he chose the variation of G as T^{-1} . After the original *Dirac hypothesis* some new ones appeared and also some generalized *theories* of gravitation admitting the variations of an effective gravitational coupling. We may single out three stages in the development of this field:

1. Study of theories and hypotheses with variations of FPC, their predictions and confrontation with experiments (1937-1977).
2. Creation of theories admitting variations of an effective gravitational constant in a particular system of units, analyses of experimental and observational data within these theories [30, 3] (1977-present).
3. Analyses of FPC variations within unified models [6, 4, 1] (present).

Within the development of the first stage from the analysis of the whole set of existed astronomical, astrophysical, geophysical and laboratory data, a conclusion was made [30, 31] that variations of

atomic constants are excluded, but variations of the effective gravitational constant in the atomic system of units do not contradict the available experimental data on the level $10^{-11} \div 10^{-12} \text{year}^{-1}$. Moreover, in [32, 30, 31] the conception was worked out that variations of constants are not absolute but depend on the system of measurements (choice of standards, units and devices using this or that fundamental interaction). Each fundamental interaction through dynamics, described by the corresponding theory, defines the system of units and the system of basic standards. Earlier reviews of some hypotheses on variations of FPC and experimental tests can be found in [3, 4]. Following Dyson (1972), we can introduce dimensionless combinations of micro- and macro-constants:

$$\begin{aligned}\alpha &= e^2/\hbar c = 7,3 \cdot 10^{-3}, & \gamma &= Gm^2/\hbar c = 5 \cdot 10^{-39}, \\ \beta &= G_F m^2 c/\hbar^3 = 9 \cdot 10^6, & \delta &= H\hbar/mc^2 = 10^{-42}, \\ \varepsilon &= \rho G/H^2 = 2 \cdot 10^{-3}, & t &= T/(e^2/mc^3) \approx 10^{40}\end{aligned}$$

We see that α , β and ε are of order 1 and γ and δ are of the order 10^{-40} . Nearly all existing hypotheses on variations of FPC may be represented as follows: **Hypothesis 1 (standard)**: α , β , γ are constant, $\delta \sim t^{-1}$, $\varepsilon \sim t$. Here we have no variations of G while δ and ε are determined by cosmological solutions. **Hypothesis 2 (Dirac)**: α , β , ε are constant, $\gamma \sim t^{-1}$, $\delta \sim t^{-1}$. Then $\dot{G}/G = 5 \cdot 10^{-11} \text{year}^{-1}$ if the age of the Universe is taken to be $T = 2 \cdot 10^{10}$ years. **Hypothesis 3 (Gamow)**: $\gamma/\alpha = Gm^2/e^2 \sim 10^{-37}$, so e^2 or α are varied, but not G , β , γ ; $\varepsilon = \text{const}$, $\alpha \sim t^{-1}$, $\delta \sim t^{-1}$. Then $\dot{\alpha}/\alpha = 10^{-10} \text{year}^{-1}$. **Hypothesis 4 (Teller)**: trying to account also for deviations of α from 1, he suggested $\alpha^{-1} = \ln \gamma^{-1}$. Then β , ε are constants, $\gamma \sim t^{-1}$, $\alpha \sim (\ln t)^{-1}$, $\delta \sim t^{-1}$

$$\dot{\alpha}/\alpha = 5 \cdot 10^{-13} \text{year}^{-1}. \quad (5)$$

The same relation for α and γ was used also by Landau, DeWitt, Staniukovich, Terasawa and others, but in approaches other than Teller's. Some other variants may be also possible, e.g. the Brans-Dicke theory with $G \sim t^{-r}$, $\rho \sim t^{-2}$, $r = [2 + 3\omega/2]^{-1}$, a combination of Gamow's and Brans-Dicke etc. [3]. **2.4.** There are different astronomical, geophysical and laboratory *data* on possible variations of FPC. **Astrophysical data:**

- a) from comparison of fine structure ($\sim \alpha^2$) and relativistic fine structure ($\sim \alpha^4$) shifts in spectra of radio galaxies, Bahcall and Schmidt (1967) obtained

$$|\dot{\alpha}/\alpha| \leq 2 \cdot 10^{-12} \text{year}^{-1}; \quad (6)$$

- b) comparing lines in optical ($\sim Ry = me^4/\hbar^2$) and radio bands of the same sources in galaxies Baum and Florentin-Nielsen (1976) got the estimate

$$|\dot{\alpha}/\alpha| \leq 10^{-13} \text{year}^{-1}, \quad (7)$$

and for extragalactic objects

$$|\dot{\alpha}/\alpha| \leq 10^{-14} \text{year}^{-1}; \quad (8)$$

- c) from observations of superfine structure in H-absorption lines of the distant radiosource Wolf et al. (1976) obtained that

$$|\alpha^2(m_e/m_p)g_p| < 2 \cdot 10^{-14}; \quad (9)$$

from these data it is seen that Hypotheses 3 and 4 are excluded. Recent data only strengthen this conclusion. Comparing the data from absorption lines of atomic and molecular transition spectra in high redshifts QSO's, Varshalovich and Potekhin, Russia, [41] obtained for $z = 2.8 - 3.1$:

$$|\dot{\alpha}/\alpha| \leq 1.6 \cdot 10^{-14} \text{ year}^{-1} \quad (10)$$

and Drinkwater et al. [43]:

$$|\dot{\alpha}/\alpha| \leq 10^{-15} \text{ year}^{-1} \text{ for } z = 0.25 \quad (11)$$

and

$$|\dot{\alpha}/\alpha| \leq 5 \cdot 10^{-16} \text{ year}^{-1} \text{ for } z = 0.68 \quad (12)$$

for a model with zero deceleration parameter and $H = 75 \text{ km} \cdot \text{s}^{-1} \cdot \text{Mpc}^{-1}$. The same conclusion is made on the bases of *geophysical data*. Indeed,

- a) α -decay of $U_{238} \rightarrow Pb_{208}$. Knowing abundancies of U_{238} and Pb_{238} in rocks and independently the age of these rocks, one obtains the limit

$$|\dot{\alpha}/\alpha| \leq 2 \cdot 10^{-13} \text{ year}^{-1}; \quad (13)$$

- b) from spontaneous fission of U_{238} such an estimation was made:

$$|\dot{\alpha}/\alpha| \leq 2, 3 \cdot 10^{-13} \text{ year}^{-1}. \quad (14)$$

- c) finally, β -decay of Re_{187} to Os_{187} gave:

$$|\dot{\alpha}/\alpha| \leq 5 \cdot 10^{-15} \text{ year}^{-1} \quad (15)$$

We must point out that all astronomical and geophysical estimations are strongly model-dependent. So, of course, it is always desirable to have *laboratory tests* of variations of FPC.

- a) Such a test was first done by the Russian group in the Committee for Standards (Kolosnitsyn, 1975). Comparing rates of two different types of clocks, one based on a Cs standard and another on a beam molecular generator, they found that

$$|\dot{\alpha}/\alpha| \leq 10^{-10} \text{ year}^{-1}. \quad (16)$$

- b) From a similar comparison of a Cs standard and SCCG (Super Conducting Cavity Generator) clocks rates Turneure et al. (1976) obtained the limit

$$|\dot{\alpha}/\alpha| \leq 4.1 \cdot 10^{-12} \text{ year}^{-1}. \quad (17)$$

- c) More recent data were obtained by J. Prestage et al. [44] by comparing mercury and H -maser clocks. Their result is

$$|\dot{\alpha}/\alpha| \leq 3.7 \cdot 10^{-14} \text{ year}^{-1}. \quad (18)$$

All these limits were placed on the fine structure constant variations. From the analysis of decay rates of K_{40} and Re_{187} , a limit on possible variations of the weak interaction constant was obtained (see approach for variations of β , e.g. in [33])

$$|\dot{\beta}/\beta| \leq 10^{-10} \text{ year}^{-1}. \quad (19)$$

But the most strict data were obtained by A. Schlyachter in 1976 (Russia) from an analysis of the ancient natural nuclear reactor data in Gabon, Oklo, because the event took place $2 \cdot 10^9$ years ago. They are the following:

$$\begin{aligned} |\dot{G}_s/G_s| &< 5 \cdot 10^{-19} \text{ year}^{-1}, \\ |\dot{\alpha}/\alpha| &< 10^{-17} \text{ year}^{-1}, \\ |\dot{G}_F/G_F| &< 2 \cdot 10^{-12} \text{ year}^{-1}. \end{aligned} \tag{20}$$

Quite recently Damour and Dyson [42] repeated this analysis in more detail and gave more cautious results:

$$|\dot{\alpha}/\alpha| \leq 5 \cdot 10^{-17} \text{ year}^{-1} \tag{21}$$

and

$$|\dot{G}_F/G_F| < 10^{-11} \text{ year}^{-1}. \tag{22}$$

So, we really see that all existing hypotheses with variations of atomic constants are excluded.

2.5. Now we still have no unified theory of all four interactions. So it is possible to construct systems of measurements based on any of these four interactions. But practically it is done now on the basis of the mostly worked out theory — on electrodynamics (more precisely on QED). Of course, it may be done also on the basis of the gravitational interaction (as it was partially earlier). Then, different units of basic physical quantities arise based on dynamics of the given interaction, i.e. the atomic (electromagnetic) second, defined via frequency of atomic transitions or the gravitational second defined by the mean Earth motion around the Sun (ephemeris time). It does not follow from anything that these two seconds are always synchronized in time and space. So, in principal they may evolve relative to each other, for example at the rate of the evolution of the Universe or at some slower rate. That is why, in general, variations of the gravitational constant are possible in the atomic system of units (c , \hbar , m are constant) and masses of all particles — in the gravitational system of units (G , \hbar , c are constant by definition). Practically we can test only the first variant since the modern basic standards are defined in the atomic system of measurements. Possible variations of FPC must be tested experimentally but for this it is necessary to have the corresponding theories admitting such variations and their certain effects. Mathematically these systems of measurement may be realized as conformally related metric forms. Arbitrary conformal transformations give us a transition to an arbitrary system of measurements. We know that scalar-tensor and multidimensional theories are corresponding frameworks for these variations. So, one of the ways to describe variable gravitational coupling is the introduction of a *scalar field* as an additional variable of the gravitational interaction. It may be done by different means (e.g. Jordan, Brans-Dicke, Canuto and others). We have suggested a variant of gravitational theory with a conformal scalar field (Higgs-type field [34, 3]) where Einstein's general relativity may be considered as a result of spontaneous symmetry breaking of conformal symmetry (Domokos, 1976) [3]. In our variant spontaneous symmetry breaking of the global gauge invariance leads to a nonsingular cosmology [35]. Besides, we may get variations of the effective gravitational constant in the atomic system of units when m , c , \hbar are constant and variations of all masses in the gravitational system of units (G , c , \hbar are constant). It is done on the basis of approximate [36] and exact cosmological solutions with local inhomogeneity [37]. The effective gravitational constant is calculated using the equations of motions. Post-Newtonian expansion is also used in order to confront the theory with existing experimental data. Among the post-Newtonian parameters the parameter f describing variations of G is included. It is

defined as

$$\frac{1}{GM} \frac{d(GM)}{dt} = fH. \quad (23)$$

According to Hellings' data [38] from the Viking mission,

$$\tilde{\gamma} - 1 = (-1.2 \pm 1.6) \cdot 10^3, \quad f = (4 \pm 8) \cdot 10^{-2}. \quad (24)$$

In the theory with a conformal Higgs field [36, 37] we obtained the following relation between f and $\tilde{\gamma}$:

$$f = 4(\tilde{\gamma} - 1). \quad (25)$$

Using Hellings' data for $\tilde{\gamma}$, we can calculate in our variant f and compare it with f from [38]. Then we get $f = (-9, 6 \pm 12, 8) \cdot 10^{-3}$ which agrees with (24) within its accuracy. We used here only Hellings' data on variations of G . But the situation with experiment and observations is not so simple. Along with [38], there are some other data [3, 4]:

1. From the growth of corals, pulsar spin down, etc. on the level

$$|\dot{G}/G| < 10^{-10} \div 10^{-11} \text{ year}^{-1}. \quad (26)$$

2. Van Flandern's positive data (though not confirmed and critisized) from the analysis of lunar mean motion around the Earth and ancient eclipses data (1976, 1981):

$$|\dot{G}/G| = (6 \pm 2) 10^{-11} \text{ year}^{-1}. \quad (27)$$

3. Reasenbergs estimates (1987) of the same Viking mission as in [38]:

$$|\dot{G}/G| < (0 \pm 2) \cdot 10^{-11} \text{ year}^{-1} \quad (28)$$

4. Hellings' result in the same form is

$$|\dot{G}/G| < (2 \pm 4) \cdot 10^{-12} \text{ year}^{-1}. \quad (29)$$

5. A result from nucleosynthesis (Acceta et al., 1992):

$$|\dot{G}/G| < (\pm 0.9) \cdot 10^{-12} \text{ year}^{-1}. \quad (30)$$

6. E.V.Pitjeva's result, Russia (1997), based on satellites and planets motion:

$$|\dot{G}/G| < (0 \pm 2) \cdot 10^{-12} \text{ year}^{-1} \quad (31)$$

As we see, there is a vivid contradiction in these results. As to other experimental or observational data, the results are rather inconclusive. The most reliable ones are based on lunar laser ranging (Muller et al, 1993 and Williams et al, 1996). They are not better than 10^{-12} per year. Here, once more we see that there is a need for corresponding theoretical and experinmental studies. Probably, future space missions like Earth SEE-satellite [39] or missions to other planets and lunar laser ranging will be a decisive step in solving the problem of temporal variations of G and determining the fates of different theories which predict them, since the greater is the time interval between successive masurements and, of course, the more precise they are, the more stringent results will be obtained. As we saw, different theoretical schemes lead to temporal variations of the effective gravitational constant:

1. Empirical models and theories of Dirac type, where G is replaced by $G(t)$.
2. Numerous scalar-tensor theories of Jordan-Brans-Dicke type where G depending on the scalar field $\sigma(t)$ appears.
3. Gravitational theories with a conformal scalar field arising in different approaches [3, 50].
4. Multidimensional unified theories in which there are dilaton fields and effective scalar fields appearing in our 4-dimensional spacetime from additional dimensions [51, 1]. They may help also in solving the problem of a variable cosmological constant from Planckian to present values.

As was shown in [4, 51, 1] temporal variations of FPC are connected with each other in *multidimensional models* of unification of interactions. So, experimental tests on $\dot{\alpha}/\alpha$ may at the same time be used for estimation of \dot{G}/G and vice versa. Moreover, variations of G are related also to the cosmological parameters ρ , Ω and q which gives opportunities of raising the precision of their determination. As variations of FPC are closely connected with the behaviour of internal scale factors, it is a direct probe of properties of extra dimensions and the corresponding theories [7, 8, 1]. **2.6. Non-Newtonian interactions, or range variations of G .** Nearly all modified theories

of gravity and unified theories predict also some deviations from the Newton law (inverse square law, ISL) or composition-dependent violations of the Equivalence Principle (EP) due to appearance of new possible massive particles (partners) [4]. Experimental data exclude the existence of these particles at nearly all ranges except less than *millimeter* and also at *meters and hundreds of meters* ranges. The most recent result in the range of 20 to 500 m was obtained by Achilli et al. using an energy storage plant experiment with gravimeters. They found a positive result for the deviation from the Newton law with the Yukawa potential strength α between 0.13 and 0.25. Of course, these results need to be verified in other independent experiments, probably in space ones [39]. In the Einstein theory G is a true constant. But, if we think that G may vary with time, then, from a relativistic point of view, it may vary with distance as well. In GR massless gravitons are mediators of the gravitational interaction, they obey second-order differential equations and interact with matter with a constant strength G . If any of these requirements is violated, we come in general to deviations from the Newton law with range (or to generalization of GR). In [5] we analyzed several classes of such theories: 1. Theories with massive gravitons like bimetric ones or theories with a Λ -term. 2. Theories with an effective gravitational constant like the general scalar-tensor ones. 3. Theories with torsion. 4. Theories with higher derivatives (4th-order equations etc.), where massive modes appear leading to short-range additional forces. 5. More elaborated theories with other mediators besides gravitons (partners), like supergravity, superstrings, M-theory etc. 6. Theories with nonlinearities induced by any known physical interactions (Born-Infeld etc.) 7. Phenomenological models where the detailed mechanism of deviation is not known (fifth or other force). In all these theories some effective or real masses appear leading to Yukawa-type deviation from the Newton law, characterized by strength and range. There exist some model-dependant estimations of these forces. The most well-known one belongs to Scherk (1979) from supergravity where the graviton is accompanied by a spin-1 partner (graviphoton) leading to an additional repulsion. Other models were suggested by Moody and Wilczek (1984) – introduction of a pseudo-scalar particle – leading to an additional attraction between macro-bodies with the range $2 \cdot 10^{-4} \text{ cm} < \lambda < 20 \text{ cm}$ and strength α from 1 to 10^{-10} in this range. Another supersymmetric model was elaborated by Fayet (1986, 1990), where a spin-1 partner of a massive graviton gives an additional repulsion in the range of the order 10^3

km and α of the order 10^{-13} . A scalar field to adjust Λ was introduced also by S. Weinberg in 1989, with a mass smaller than $10^{-3}\text{eV}/c^2$, or a range greater than 0.1 mm. One more variant was suggested by Peccei, Sola and Wetterich (1987) leading to additional attraction with a range smaller than 10 km. Some p -brane models also predict non-Newtonian additional interactions in the mm range, what is intensively discussed nowadays. About PPN parameters for multidimensional models with p -branes see below. **2.7. SEE - Project** We saw that there are three problems connected with G . There is a promising new multi-purpose space experiment SEE - Satellite Energy Exchange [39], which addresses all these problems and may be more effective in solving them than other laboratory or space experiments. This experiment is based on a limited 3-body problem of celestial mechanics: small and large masses in a drag-free satellite and the Earth. Unique horse-shoe orbits, which are effectively one-dimensional, are used in it. The aims of the SEE-project are to measure: Inverse Square law (ISL) and Equivalence Principle (EP) at ranges of meters and the Earth radius, G -dot and the absolute value of G with unprecedented accuracies. We studied some aspects of the SEE-project [57] : 1. Wide range of trajectories with the aim of finding optimal ones: - circular in spherical field; - the same plus Earth quadrupole modes; - elliptic with eccentricity less than 0.05. 2. Estimations of other celestial bodies influence. 3. Estimation of relative influence of trajectories to changes in G and α . 4. Modelling measurement procedures for G and α by different methods, for different ranges and for different satellite altitudes: optimal - 1500 km, ISS free flying platform - 500 km and also for 3000 km. 5. Estimations of some sources of errors: - radial oscillations of the shepherd's surface; - longitudinal oscillations of the capsule; - transversal oscillations of the capsule; - shepherd's nonsphericity; - limits on the quadrupole moment of the shepherd; - limits on admissible charges and time scales of charging by high energy particles etc. 6. Error budgets for G , G -dot and $G(r)$. The general conclusion is that the SEE-project may really improve our knowledge of these values by 3-4 orders better than we have nowadays.

3. Multidimensional Models

The history of the multidimensional approach begins with the well-known papers of T.K. Kaluza and O. Klein on 5-dimensional theories which opened an interest to investigations in multidimensional gravity. These ideas were continued by P. Jordan who suggested to consider the more general case $g_{55} \neq \text{const}$ leading to a theory with an additional scalar field. They were in some sense a source of inspiration for C. Brans and R.H. Dicke in their well-known work on a scalar-tensor gravitational theory. After their work a lot of investigations have been performed using material or fundamental scalar fields, both conformal and non-conformal (see details in [3]). A revival of ideas of many dimensions started in the 70's and continues now. It is completely due to the development of unified theories. In the 70's an interest to multidimensional gravitational models was stimulated mainly by (i) the ideas of gauge theories leading to a non-Abelian generalization of the Kaluza-Klein approach and (ii) by supergravitational theories. In the 80's the supergravitational theories were "replaced" by superstring models. Now it is heated by expectations connected with the overall M-theory. In all these theories, 4-dimensional gravitational models with extra fields were obtained from some multidimensional model by dimensional reduction based on the decomposition of the manifold

$$M = M^4 \times M_{\text{int}}, \quad (32)$$

where M^4 is a 4-dimensional manifold and M_{int} is some internal manifold (mostly considered to be compact). The earlier papers on multidimensional gravity and cosmology dealt with multi-

dimensional Einstein equations and with a block-diagonal cosmological or spherically symmetric metric defined on the manifold $M = \mathbb{R} \times M_0 \times \dots \times M_n$ of the form

$$g = -dt \otimes dt + \sum_{r=0}^n a_r^2(t) g^r \quad (33)$$

where (M_r, g^r) are Einstein spaces, $r = 0, \dots, n$. In some of them a cosmological constant and simple scalar fields were also used [15]. Such models are usually reduced to pseudo-Euclidean Toda-like systems with the Lagrangian

$$L = \frac{1}{2} G_{ij} \dot{x}^i \dot{x}^j - \sum_{k=1}^m A_k e^{u_k^i x^i} \quad (34)$$

and the zero-energy constraint $E = 0$. It should be noted that pseudo-Euclidean Toda-like systems are not well-studied yet. There exists a special class of equations of state that gives rise to Euclidean Toda models [9]. Cosmological solutions are closely related to solutions with spherical symmetry [16]. Moreover, the scheme of obtaining the latter is very similar to the cosmological approach [1]. The first multidimensional generalization of such type was considered by D. Kramer and rediscovered by A.I. Legkii, D.J. Gross and M.J. Perry (and also by Davidson and Owen). In [52] the Schwarzschild solution was generalized to the case of n internal Ricci-flat spaces and it was shown that a black hole configuration takes place when the scale factors of internal spaces are constants. It was shown there also that a minimally coupled scalar field is incompatible with the existence of black holes. In [10] an analogous generalization of the Tangherlini solution was obtained, and an investigation of singularities was performed in [26]. These solutions were also generalized to the electrovacuum case with and without a scalar field [11, 13, 12]. Here, it was also proved that BHs exist only when a scalar field is switched off. Deviations from the Newton and Coulomb laws were obtained depending on mass, charge and number of dimensions. In [12] spherically symmetric solutions were obtained for a system of scalar and electromagnetic fields with a dilaton-type interaction and also deviations from the Coulomb law were calculated depending on charge, mass, number of dimensions and dilaton coupling. Multidimensional dilatonic black holes were singled out. A theorem was proved in [12] that “cuts” all non-black-hole configurations as being unstable under even monopole perturbations. In [14] the extremely charged dilatonic black hole solution was generalized to a multicenter (Majumdar-Papapetrou) case when the cosmological constant is non-zero. We note that for $D = 4$ the pioneering Majumdar-Papapetrou solutions with a conformal scalar field and an electromagnetic field were considered in [24]. At present there exists a special interest to the so-called M- and F-theories etc. These theories are “supermembrane” analogues of the superstring models in $D = 11, 12$ etc. The low-energy limit of these theories leads to models governed by the Lagrangian

$$\mathcal{L} = R[g] - h_{\alpha\beta} g^{MN} \partial_M \varphi^\alpha \partial_N \varphi^\beta - \sum_{a \in \Delta} \frac{\theta_a}{n_a!} \exp[2\lambda_a(\varphi)] (F^a)^2, \quad (35)$$

where g is a metric, $F^a = dA^a$ are forms of rank $F^a = n_a$, and φ^α are scalar fields. In [46] it was shown that, after dimensional reduction on the manifold $M_0 \times M_1 \times \dots \times M_n$ and when the composite p -brane ansatz is considered, the problem is reduced to the gravitating self-interacting σ -model with certain constraints. For electric p -branes see also [17, 18, 20] (in [20] the composite electric case was considered). This representation may be considered as a powerful tool for obtaining different solutions with intersecting p -branes (analogs of membranes). In [46, 29] Majumdar-Papapetrou type solutions were obtained (for the non-composite electric

case see [17, 18] and for the composite electric case see [20]). These solutions correspond to Ricci-flat (M_i, g^i) , $i = 1, \dots, n$ and were generalized to the case of Einstein internal spaces [46]. The obtained solutions take place when certain *orthogonality relations* (on couplings parameters, dimensions of “branes”, total dimension) are imposed. In this situation a class of cosmological and spherically symmetric solutions was obtained [27]. Special cases were also considered in [22]. Solutions with a horizon were considered in detail in [21, 27]. In [21, 28] some propositions related to (i) interconnection between the Hawking temperature and the singularity behaviour, and (ii) to multitemporal configurations were proved. It should be noted that multidimensional and multitemporal generalizations of the Schwarzschild and Tangherlini solutions were considered in [13, 25], where the generalized Newton formulas in a multitemporal case were obtained. We note also that there exists a large variety of Toda solutions (open or closed) when certain intersection rules are satisfied [27]. We continued our investigations of p -brane solutions based on the sigma-model approach in [46, 18, 20]. (For the pure gravitational sector see [17, 45, 46].) We found a family of solutions depending on one variable describing the (cosmological or spherically symmetric) “evolution” of $(n + 1)$ Einstein spaces in the theory with several scalar fields and forms. When an electro-magnetic composite p -brane ansatz is adopted, the field equations are reduced to the equations for a Toda-like system. In the case when n “internal” spaces are Ricci-flat, one space M_0 has a non-zero curvature, and all p -branes do not “live” in M_0 , we found a family of solutions to the equations of motion (equivalent to equations for Toda-like Lagrangian with zero-energy constraint [27]) if certain *block-orthogonality relations* on p -brane vectors U^s are imposed. These solutions generalize the solutions from [27] with an orthogonal set of vectors U^s . A special class of “block-orthogonal” solutions (with coinciding parameters ν_s inside blocks) was considered earlier in [28]. We considered a subclass of spherically symmetric solutions. This subclass contains non-extremal p -brane black holes for zero values of “Kasner-like” parameters. A relation for the Hawking temperature was presented (in the black hole case). We also calculated the Post-Newtonian Parameters β and γ (Eddington parameters) for general spherically symmetric solutions and black holes in particular [54]. These parameters depending on p -brane charges, their worldvolume dimensions, dilaton couplings and number of dimensions may be useful for possible physical applications. Some specific models in classical and quantum multidimensional cases with p -branes were analysed in [47]. Exact solutions for the system of scalar fields and fields of forms with a dilatonic type interactions for *generalized intersection rules* were studied in [48], where the PPN parameters were also calculated. Finally, a *stability* analysis for solutions with p -branes was carried out [49]. It was shown there that for some simple p -brane systems multidimensional black branes are stable under monopole perturbations while other (non-BH) spherically symmetric solutions turned out to be unstable.

Acknowledgement

The author is very grateful to Don Strayer, Ulf Israelsson and Monica King for their hospitality during his stay in Solvang. The work was supported in part by the NASA/SEE project and CONACYT, Mexico

References

- [1] V.N. Melnikov, “Multidimensional Classical and Quantum Cosmology and Gravitation. Exact Solutions and Variations of Constants.” CBPF-NF-051/93, Rio de Janeiro, 1993;
V.N. Melnikov, in: “Cosmology and Gravitation”, ed. M. Novello, Editions Frontieres, Singapore, 1994, p. 147.

- [2] V.N. Melnikov, “Multidimensional Cosmology and Gravitation”, CBPF-MO-002/95, Rio de Janeiro, 1995, 210 p.;
V.N. Melnikov. In: *Cosmology and Gravitation. II*, ed. M. Novello, Editions Frontieres, Singapore, 1996, p. 465.
- [3] K.P. Staniukovich and V.N. Melnikov, “Hydrodynamics, Fields and Constants in the Theory of Gravitation”, Energoatomizdat, Moscow, 1983, 256 pp. (in Russian).
- [4] V.N. Melnikov, *Int. J. Theor. Phys.* **33**, 1569 (1994).
- [5] V. de Sabbata, V.N. Melnikov and P.I. Pronin, *Prog. Theor. Phys.* **88**, 623 (1992).
- [6] V.N. Melnikov. In: “Gravitational Measurements, Fundamental Metrology and Constants”, eds. V. de Sabbata and V.N. Melnikov, Kluwer Academic Publ., Dordrecht, 1988, p. 283.
- [7] V.D. Ivashchuk and V.N. Melnikov, *Nuovo Cimento* **B 102**, 131 (1988).
- [8] K.A. Bronnikov, V.D. Ivashchuk and V.N. Melnikov, *Nuovo Cimento* **B 102**, 209 (1988).
- [9] V.R. Gavrilo, V.D. Ivashchuk and V.N. Melnikov, “Integrable Pseudo-euclidean Toda-like Systems in Multidimensional Cosmology with Multicomponent Perfect Fluid”, *J. Math. Phys.* **36**, 5829 (1995).
- [10] S.B. Fadeev, V.D. Ivashchuk and V.N. Melnikov, *Phys. Lett. A* **161**, 98 (1991).
- [11] S.B. Fadeev, V.D. Ivashchuk and V.N. Melnikov, *Chinese Phys. Lett.* **8**, 439 (1991).
- [12] K.A. Bronnikov and V.N. Melnikov, *Annals of Physics (N.Y.)* **239**, 40 (1995).
- [13] V.D. Ivashchuk and V.N. Melnikov, *Class. Quantum Grav.*, **11**, 1793 (1994).
- [14] V.D. Ivashchuk and V.N. Melnikov, “Extremal Dilatonic Black Holes in String-like Model with Cosmological Term”, *Phys. Lett. B* **384**, 58 (1996).
- [15] U. Bleyer, V.D. Ivashchuk, V.N. Melnikov and A.I. Zhuk, “Multidimensional Classical and Quantum Wormholes in Models with Cosmological Constant”, gr-qc/9405020; *Nucl. Phys. B* **429**, 117 (1994).
- [16] V.D. Ivashchuk and V.N. Melnikov, “Multidimensional Gravity with Einstein Internal Spaces”, hep-th/9612054; *Grav. & Cosmol.* **2**, 177 (1996).
- [17] V.D. Ivashchuk and V.N. Melnikov, “Intersecting p -brane Solutions in Multidimensional Gravity and M-Theory”, hep-th/9612089; *Grav. & Cosmol.* **2**, No 4, 297 (1996).
- [18] V.D. Ivashchuk and V.N. Melnikov, *Phys. Lett. B* **403**, 23 (1997).
- [19] V.D. Ivashchuk and V.N. Melnikov, “Sigma-Model for Generalized Composite p -branes”, hep-th/9705036; *Class. Quant. Grav.* **14**, 11, 3001 (1997).
- [20] V.D. Ivashchuk, M. Rainer and V.N. Melnikov, “Multidimensional Sigma-Models with Composite Electric p -branes”, gr-qc/9705005; *Gravit. & Cosm.* **4**, No. 1 (13) (1998).
- [21] K.A. Bronnikov, V.D. Ivashchuk and V.N. Melnikov, “The Reissner-Nordström Problem for Intersecting Electric and Magnetic p -branes”, gr-qc/9710054; *Grav. & Cosmol.* **3**, 203 (1997).
- [22] K.A. Bronnikov, U. Kasper and M. Rainer, “Intersecting Electric and Magnetic p -Branes: Spherically Symmetric Solutions”, gr-qc/9708058.

- [23] M.A. Grebeniuk, V.D. Ivashchuk and V.N. Melnikov, “Multidimensional Cosmology for Intersecting p -branes with Static Internal Spaces”, *Grav. & Cosmol.*, **4**, No 2(14), 145 (1998).
- [24] N.M. Bocharova, K.A. Bronnikov and V.N. Melnikov, *Vestnik MGU (Moscow Univ.)*, **6**, 706 (1970)(in Russian, English transl.: Moscow Univ. Phys. Bull., **25**, 6, 80 (1970)) — the first MP-type solution with a conformal scalar field;
K.A. Bronnikov, *Acta Phys. Polonica*, **B4**, 251 (1973);
K.A. Bronnikov and V.N. Melnikov, in *Problems of Theory of Gravitation and Elementary Particles*, **5**, 80 (1974) (in Russian) — the first MP-type solution with conformal scalar and electromagnetic fields.
- [25] V.D. Ivashchuk and V.N. Melnikov, *Int. J. Mod. Phys. D* **4**, 167 (1995).
- [26] V.D. Ivashchuk and V.N. Melnikov, “On Singular Solutions in Multidimensional Gravity”, hep-th/9612089; *Grav. and Cosmol.* **1**, 204 (1996).
- [27] V.D. Ivashchuk and V.N. Melnikov, “Multidimensional Classical and Quantum Cosmology with Intersecting p -branes”, hep-th/9708157; *J. Math. Phys.*, **39**, 2866 (1998).
- [28] K.A. Bronnikov, “Block-orthogonal Brane Systems, Black Holes and Wormholes”, hep-th/9710207; *Grav. and Cosmol.* **4**, No 2 (14), (1998).
- [29] V.D. Ivashchuk and V.N. Melnikov, “Mudjumdar-Papapetrou Type Solutions in Sigma-model and Intersecting p -branes”, hep-th/9702121, *Class. Quant. Grav.* **16**, 849 (1999).
- [30] V.N. Melnikov and K.P. Staniukovich. In: “Problems of Gravitation and Elementary Particle Theory (PGEPT)”, Atomizdat, Moscow, 1978, v.9, p.3 (in Russian).
- [31] N.A. Zaitsev and V.N. Melnikov. In: PGEPT, 1979, v.10, p.131.
- [32] V. Canuto et al. *Phys. Rev.* **D 16**, 1643 (1977).
- [33] M. Novello and P. Rotelli, *J. Phys. A* **5**, 1488 (1972).
- [34] K.A. Bronnikov, V.N. Melnikov and K.P. Staniukovich. ITP-68-69, Kiev, 1968.
- [35] V.N. Melnikov. *Dokl. Acad. Nauk* **246**, N 6, 1351 (1979);
V.N. Melnikov and S.V. Orlov, *Phys.Lett.* **70 A**, N4, 263 (1979).
- [36] V.N. Melnikov and A.G. Radynov. In: PGEPT, 1984, v.14, p.73.
- [37] V.N. Melnikov and A.G. Radynov. In: “On Relativity Theory”, Singapore, WS, 1985, v.2, p.196.
- [38] R. Hellings, *Phys. Rev. Lett.* **51**, 1609 (1983).
- [39] A. Sanders and W. Deeds. *Phys. Rev.* **D 46**, 480 (1992).
- [40] J.D. Barrow, gr-qc/9711084.
- [41] D.A. Varshalovich and A.Y. Potekhin. *Space Sci. Rev.* **74**, 259 (1995); *Pis'ma Atron. Zh.* **22**, 3 (1996); *Astron. Lett.*, **22**, 6 (1996).
- [42] T. Damour and F. Dyson. *Nucl. Phys.*, **B 480**, 37 (1996).
- [43] M. Drinkwater et al., *MNRAS*, 1999, November, astro-ph/9711290.
- [44] J.D. Prestage et al., *Phys. Rev. Lett.* **74**, 3511 (1995).

- [45] V.D. Ivashchuk and V.N. Melnikov, *J. Math. Phys.* **40**, 6568 (1999), gr-qc/9901001.
- [46] S. Cotsakis, V.D. Ivashchuk and V.N. Melnikov. *Grav. & Cosm.* **5**, 52 (1999).
- [47] M.A. Grebeniuk, V.D. Ivashchuk, V.N. Melnikov and R. Triay, *Grav. & Cosmol.* **5**, 229 (1999).
- [48] V.D. Ivashchuk and V.N. Melnikov, Proc. 2nd Int. Gamov Conf., Odessa, Ukraine, 1999; *Grav. & Cosmol.* **5**, 313 (1999), hep-th/9910041; *Class.Quant.Grav.*, 2000, to appear.
- [49] K.A. Bronnikov and V.N. Melnikov. *Grav. & Cosmol.* **5**, 306 (1999); *Nucl.Phys.*, 2000, to appear.
- [50] V.N. Melnikov et al., *GRG* **17**, 63 (1985).
- [51] V.N. Melnikov. In: "Results of Science and Technology. Gravitation and Cosmology". Ed.: V.N. Melnikov, 1991, v.1, p.49 (in Russian).
- [52] K.A. Bronnikov and V.D. Ivashchuk. In: Abstr. 8th Sov. Grav. Conf., Erevan, EGU, 1988, p.156.
- [53] *Measurement Science and Technology*, **10**, (1999).
- [54] V.D. Ivashchuk and V.N. Melnikov. In: Lecture Notes in Physics, vol.537. Mathematical and Quantum Aspects of Relativity and Cosmology. Eds.: S.Cotsakis and G.Gibbons. Proc. 2 Samos Meeting on Cosmology, Geometry and Relativity. Springer, Berlin, 2000, p.214.
- [55] E.V. Pitjeva. In: Dynamics and Astrometry of Natural and Artificial Celestial Bodies. Kluwer Acad. Publ., Netherlands, 1997, p. 251.
- [56] J.H. Gundlach and S.M. Merkowitz, gr-qc/0006043.
- [57] A.D. Alexeev, K.A. Bronnikov, N.I. Kolosnitsyn, M.Yu. Konstantinov, V.N.Melnikov and A.G.Radynov. *Izmeritelnaya tekhnika*, 1993, N 8, p.6; N 9, p.3; N 10, p.6; 1994, N1, p.3. *Int. J. Mod. Phys.*, 1994, **D 3**, N 4, p.773. P.N. Antonyuk, K.A. Bronnikov and V.N. Melnikov. *Astron.Lett.*, 1994, **20**, N 1, p.59. *Grav. Cosm.*, 1997, **3**, N 4(12). K.A. Bronnikov, M.Yu. Konstantinov and V.N. Melnikov, *Grav. Cosm.*, 1996, **2**, N 4(8), p.361. *Izmerit. Tekhnika*, 1996, N 5, p.3. A.D. Alexeev,..., V.N.Melnikov et al. Ibid., 1997, N 10, p.3. *Grav.Cosm.*, 1999, **5**, N1(17), p.67. A.J.Sanders,..., V.N.Melnikov et al. Ibid, 1997, **3**, p.287. *Meas.Sci.Technol.*, 1999, **10**, p.514. *Class.Quant.Grav.*, 2000, **17**, N 1. V.N. Melnikov. *Science in Russia*, 2000, N 6, November.

Plans for a SEE (Satellite Energy Exchange) Mission

Al Sanders
University of Tennessee

A SEE mission is designed to make extremely accurate measurements on fundamental gravitation by observing the orbital perturbation of unconstrained orbiting test bodies in a femto- to atto-g environment. A SEE mission will use novel and original test-body dynamics.

Gravitation is the missing link in unification theory. The broad objective of a SEE mission is to support development of gravity theory and unification theory by carrying out sensitive gravitational tests capable of discriminating among alternative theories. The SEE satellite will provide *controlled* experiments with very fine accuracy, which can discriminate among various possible unified theories.

A SEE mission would entail launching a dedicated satellite, the heart of which would be an experimental chamber in which two or three test bodies--one large "Shepherd" and one or two small "Particles"--would float freely, experiencing only each other's gravity and that of the Earth and other bodies in the solar system. Observation of the mutual perturbations of the test bodies will provide the required data for the tests and measurements of a SEE mission.

SEE differs from other proposed gravity missions in six important respects:

1. The focus of SEE is post-Einsteinian; it is not limited only to specific tests of general relativity. SEE is truly a next-generation gravity mission that will measure or test a number of links of gravitation and unified theories.
2. SEE is multi-purpose and observational in approach; it is not designed to test one or two hypotheses using a single-purpose instrument.
3. The SEE satellite uses new and unique test-body dynamics, based on the limited three-body problem of celestial mechanics.
4. SEE uses extremely advanced passive technology for most aspects of satellite control and data acquisition.
5. The SEE Satellite design is holistic; it is not a combination of modules having separate and possibly competing requirements.
6. Because of reliance on passive technology, the life of a SEE mission can be extended indefinitely if needed. Since there is no reliance on liquefied gas or consumable fuel, the SEE satellite can continue to take vast amounts of data as long as the data continue to be of high scientific value.

A SEE mission has six measurement goals:

1. Test for violation of the Equivalence-Principle (EP) by Inverse-Square-Law (ISL) violations (EP/ISL) at distances on the order of meters.
2. Test for EP/ISL violation at distances on the order of the radius of the Earth.
3. Test for violation of the Equivalence-Principle (EP) by Composition Dependent (CD) violations (EP/CD) at distances on the order of meters.
4. Test for (EP/CD) violations at distances on the order of the radius of the Earth.

5. Measure the absolute value of the Gravitational constant G .
6. Test for non-zero value of $G\text{-dot}$, the time derivative of G .

SEE will be better by far than any existing and/or planned experiments in the measurement of G , the test for $G\text{-dot}$, and the tests for EP/ISL violation at both distances. Our long-range test for EP/CD will be 2-3 orders better than the existing tests, albeit at somewhat lower accuracies than those of proposed experiments, and will thus be at sufficient accuracy to bolster confidence in the results of other experiments, assuming that their accuracies goals are realized and that their results are correct.

Concerning $G\text{-dot}$, few things could be more significant scientifically than discovering that a fundamental "constant" of Nature is not constant; few things could do more to invigorate interest in the new theories, most of which do in fact predict time variation of G and other fundamental "constants." A finding of non-zero $G\text{-dot}$ would of course require extensions of general relativity, since it assumes a constant value of G . More broadly, this would clearly mark the boundaries where general relativity is valid, and specify the onset of new physics.

Tests of the equivalence principle, both by inverse-square-law (ISL) tests and composition-dependent (CD) tests, are extremely important because of the far-reaching and profound consequences of any violation. Any apparent violation could be interpreted most readily as evidence of the existence of a new super-weak force, presumably of short range and therefore mediated by a massive particle--i.e., α in terms of a Yukawa-type potential.

The motivation for an improved determination of the gravitational constant G is two-fold: first, simply that it is very poorly known in relation to all other fundamental constants; second, that various theoretical methods for calculating the value of G are now becoming available, thus supplying tests of these theories--but only if the experimental value of G is sufficiently accurate. Most importantly, various multi-dimensional theories produce relations between fundamental constants, and it is hoped that the set of constants of some multi-dimensional theory will be proven to correspond to the known fundamental constants, and will yield extremely accurate values of poorly-known constants via those which are most precisely known.

A SEE mission also has the potential of testing for possible spatial variation of G according to the direction in which the gravitational force is applied.

A SEE mission utilizes the rather paradoxical relative motion of two independently-orbiting test bodies during a SEE encounter. This special case of the restricted three-body problem was first discovered by George Darwin at the end of the 19th century. It is valuable for detailed analysis of gravitational interactions because it provides a wide variation of separations between the test bodies and a relatively long "hang time". The bulk of the scientific investigation on a SEE mission would entail precise analyses of the relative motion of the two test bodies--the large "Shepherd" and the small "Particle"--during a number of SEE encounters, to deduce the relative interactions of the test bodies. In addition, ground tracking of the satellite will provide precise long-term orbit information for deducing the long-term perturbations of the Shepherd.

The SEE (Satellite Energy Exchange) concept is rooted in the tradition of orbital-perturbation analysis. Thus, we seek to make very precise measurements of small effects, by allowing time to magnify them naturally. As with all such analyses--from the discovery of Uranus to the explanation of the perihelion precession of Mercury--our analysis methods will disentangle the sought-after effects from each other and from various background effects (such as the influence of the Moon and of the Earth's harmonics). Although in some cases the background effects may be large, they will generally be calculable and--since SEE provides for *controlled* experiments--we will often have the added luxury of being able to choose the phases of the effects under investigation, relative to each other and relative to the unwanted background effects.

Finally, although we begin with specific hypotheses, if neither these nor other existing hypotheses provide satisfactory fits to the data, and if exhaustive searches for further systematic errors prove fruitless, then this circumstance will invite theorists to posit new hypotheses.

The problems and opportunities entailed in the control of a satellite and acquisition of data have been carefully re-thought from first principles by the SEE team, with the result that several very novel techniques have been developed. These techniques have been gradually integrated, over a period of 10 years, into a truly holistic design concept for the SEE satellite. Among these techniques are means of (1) non-contact absolute measurement of distance with sub-micron precision at large stand-off distances, (2) passive cryogenic cooling for periods of years, (3) station-keeping thrust for drag-free operation with virtually no expenditure of energy, and (4) making the satellite itself essentially "gravitationally invisible" to the test bodies. U.S. and international patents have been granted for several of these technologies.

Helium Constraint for the **STEP** Experiment using Silica Aerogel

SATELLITE **T**EST OF THE **E**QUIVALENCE **P**RINCIPLE **STEP**

Rodney Torii

W.W. Hansen Experimental Physics Laboratory
Stanford University, Stanford, CA 94305-4085

Satellite Test of the Equivalence Principle

STEP SMEX SCIENCE TEAM

- Francis Everitt PI Stanford
- Paul Worden Co-PI Stanford
- John Anderson Co-I JPL
- Hansjoerg Dittus Co-I Bremen
- Nick Lockerbie Co-I Strathclyde
- John Mester Co-I Stanford
- Tim Sumner Co-I Imperial College
- Rodney Torii Co-I Stanford
- Stefano Vitale Co-I Trento

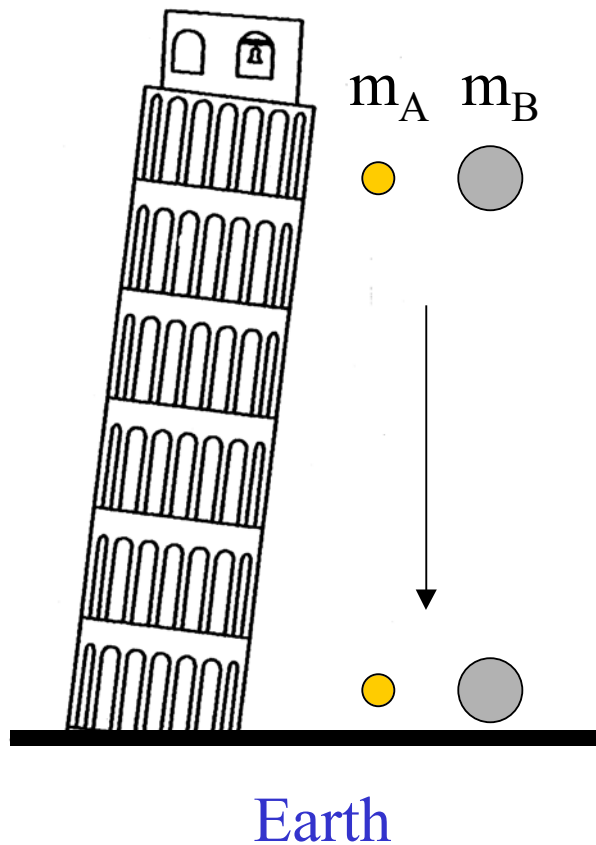
Satellite Test of the Equivalence Principle

STEP AEROGEL TEST

- Suwen Wang Stanford
- Rita Dolesi Trento
- Don Strayer JPL
- Steve Jones JPL
- Guy Man JPL

Weak Equivalence Principle

UNIVERSALITY OF FREE FALL (UFF)



- **UFF**: Observed Fact That **All** Bodies Fall to Ground w/ **Same** Acceleration
 - Mass (Size)
 - **COMPOSITION** (A, B, C, ... X)
 - Newtonian Physics
 - Gravitational Mass m_G
 - Inertial Mass m_I (2nd Law)
- $m_G \propto m_I$
- UNIVERSAL Constant of Proportionality

$$\left(\frac{m_G}{m_I} \right)_A = \left(\frac{m_G}{m_I} \right)_B = \left(\frac{m_G}{m_I} \right)_C \dots = \left(\frac{m_G}{m_I} \right)_X$$

Weak **E**quivalence **P**inciple (**EP**)

THEORETICAL SIGNIFICANCE

- Theories Of Quantum Gravity Introduce **C**omposition **D**ependent (**CD**) Forces That Violate The Equivalence Principle (*e.g., 10^{-14} - 10^{-23})
 - Use **EP** Test To Test Theories Of Quantum Gravity
- **EP** Violation
 - New Fundamental Force “Fifth Force”
 - Fundamental Effect on General Relativity
- No **EP** Violation
 - Limit Possible Paths To Quantum Gravity

*T. Damour and A.M. Polykov, Nucl. Phys. B 423, 532 (1994)

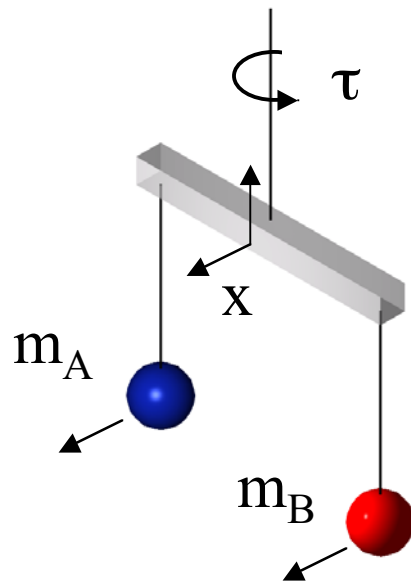
Weak Equivalence Principle

MODERN CD **UFF** EXPERIMENTS

TORSION BALANCE

Composition **A** \neq **B**

Search For **CD** Force



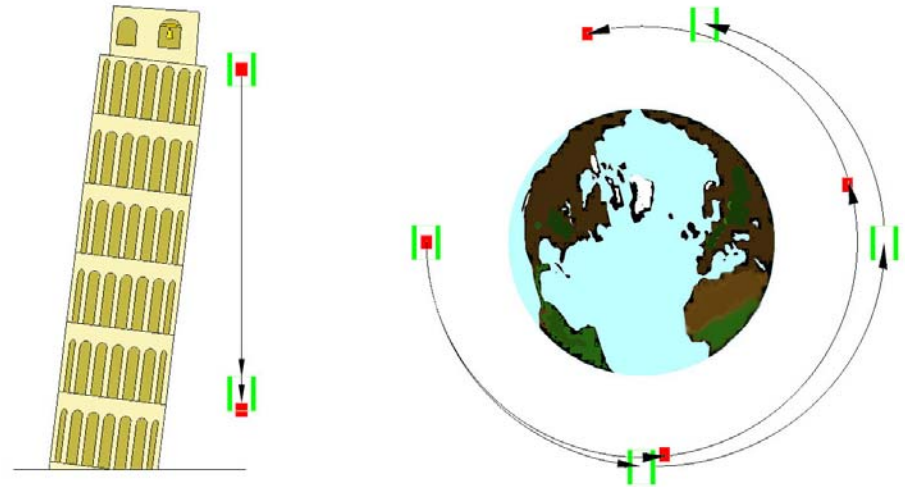
Source

- **Dicke, et. al.,**
 - 3×10^{-11} **1964**
 - **Sun Source**
 - **EP Violation 24 hr Period**
- **Adelberger, et. al.,**
 - 2×10^{-12} **1994**
 - 1×10^{-13} **1999**
 - **Turntable 1000 s Period**
- **STEP**
 - 10^{-18} **2004 ?**

Satellite Test of the Equivalence Principle STEP EXPERIMENT CONCEPT*

EP Test in Space

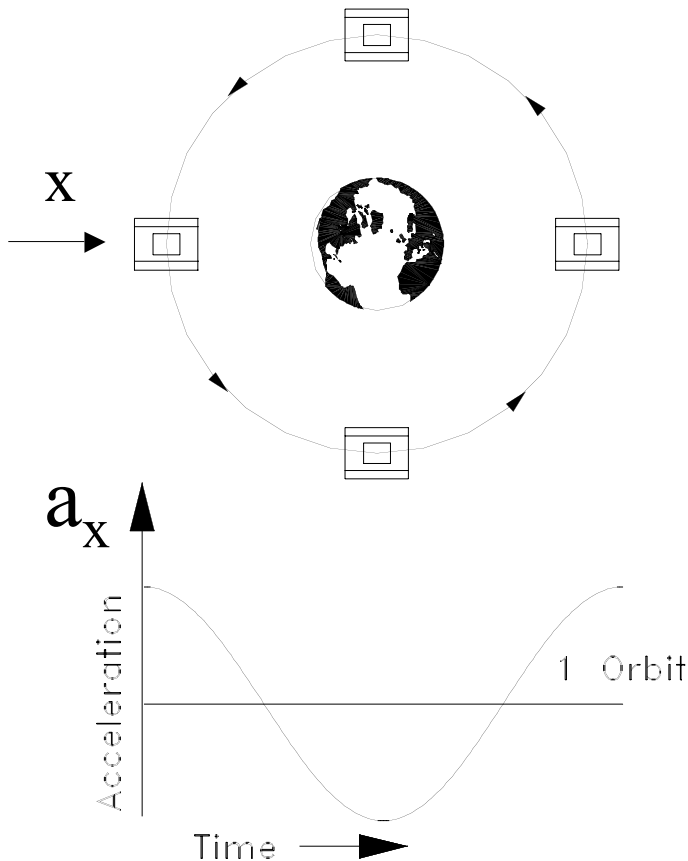
- **STEP**
 - NASA SMEX Proposal
 - 10^{-18} 2004
- **μSCOPE**
 - CNES (France) Funded
 - 10^{-15} 2004



*P.W. Worden, Jr., Ph.D. Thesis, Stanford University, Stanford, CA (1976).

Satellite Test of the Equivalence Principle

STEP INSTRUMENT DESIGN



- Single Axis **1 DOF** Detection
 - EP Violation Orbital Frequency
 - Signal Phase and Bandwidth
- **Differential** Measurement
 - Reject Non-EP Disturbances Common To Both Masses
- Spacecraft\Platform Noise
 - **Drag-Free** Technology (GP-B)
- Cryogenics
 - Test Mass Brownian Motion, Superconductors, DC SQUID

Satellite Test of the Equivalence Principle

STEP EXPERIMENT GOAL

- 10^{-18} EP Test

- Earth Free Fall Acceleration a g_0
- Differential Acceleration δa $10^{-18} g_0$
- Differential Acceleration Sensitivity $4 \times 10^{-19} g_0$
 - Displacement Sensitivity 10^{-13} m
 - Natural Frequency 10^{-3} Hz
- Residual Gravity Gradient Acceleration $1 \times 10^{-16} g_0$
 - Align Centers Of Mass 10^{-9} m
- Residual Spacecraft Acceleration $2 \times 10^{-15} g_0$
 - Displacement Sensitivity $5 \times 10^{-10} \text{ m}$ $5 \times 10^{-11} \text{ m}$
 - Natural Frequency 10^{-3} Hz $3 \times 10^{-3} \text{ Hz}$

Satellite Test of the Equivalence Principle

STEP NOISE SOURCES

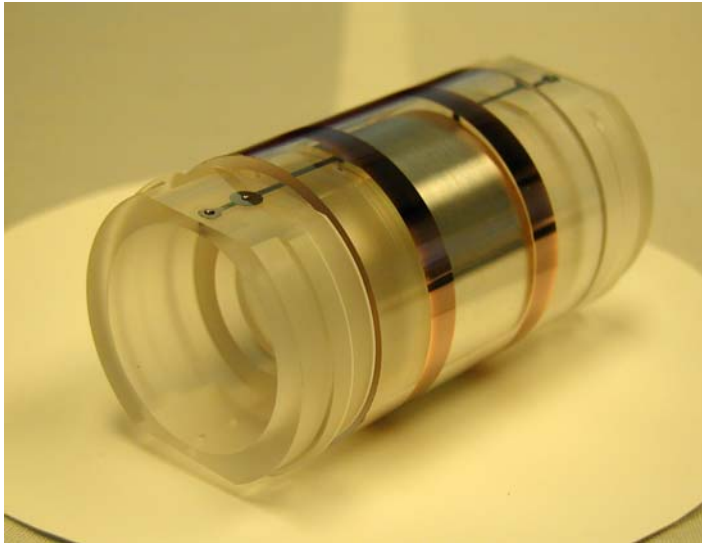
- **Noise Limiting Performance of Instrument in Ideal Environment**
- **Noise Due to Environment Forces Acting on Instrument**
- **Intrinsic Noise of the Instrument**
 - Thermal Noise Limit of Mass-Spring Accelerometer with Finite Q^*
 - Position Sensor Noise
 - Intrinsic Noise of DC SQUID and Circuit Losses
 - Spring Noise
 - “Patch Effect” Forces and Losses

*H.A. Chan and H.J. Paik, Phys. Rev. D **35**, 3551 (1987).

STEP Science Instrument Development

INNER ACCELEROMETER

Accelerometer



- Prototype Accelerometer
 - 1/2 Differential Accelerometer
 - Cryogenic
 - Prototype Components
 - Test Mass
 - Magnetic Bearing System
 - SQUID Readout System
 - Electrostatic Positioning System

Construction and Test of a Spin Source for Spin-Mass Coupling Experiment

Ho Jung Paik, M. Vol Moody, and Jonghee Lee

Department of Physics, University of Maryland, College Park, MD 20742

A spin source that can be modulated to a significant fraction of saturation is desired for an experiment searching for spin-mass interaction. We have successfully fabricated such a spin source with alternating sections of ferromagnetic material (Magnifer) and copper in toroidal geometry. Superconducting coils were wound over these materials to magnetize the spin source. The entire source was wrapped with a superconducting shield. This spin source has been tested extensively at 4.2 K. By measuring the inductances of the coils, we have verified that the source works as designed, i.e., the magnetic field generated by the magnetizing coil feeds through both materials, aligning the spin in Magnifer. We have shown that magnetization in Magnifer can be modulated with an amplitude of 7.3×10^4 A/m at the signal frequency of 0.01 Hz. The corresponding spin density, 3.9×10^{21} cm⁻³, represents 17 % of the maximum spin saturation in Magnifer. The heat generated in the spin source due to eddy current damping is < 0.5 mW.

1. Introduction

One of the most important unresolved issues in the Standard Model of particle physics is the “strong CP problem.” Peccei and Quinn (1977) developed an attractive explanation for this phenomenon two decades ago, but experimentalists have so far failed to test it. One of the most important results of the theory is the prediction of the existence of the axion, which mediates a force between mass and intrinsic spin (Weinberg, 1978; Wilczek, 1978). Confirmation of this prediction would have a major impact on our understanding of the universe.

To improve the sensitivity for the spin-mass coupling by several orders of magnitude, we have designed an experiment in which superconducting accelerometer technology is combined with other benefits of low temperature environment (Paik *et al.*, 1999). Superconducting magnetic levitation allows extremely soft, low-loss, suspension of the test masses, and low pressure achievable in cryogenic environment permits a very low gas-limited damping of the resonance quality factor, greatly enhancing the sensitivity of the accelerometer. Cryogenic temperatures permit the use of near perfect superconducting shield against electromagnetic interference.

Our laboratory has the world’s most sensitive operating differential accelerometer. The superconducting gravity gradiometer that we developed reached an operational level of 4×10^{-12} m s⁻² Hz^{-1/2}, 100 times more sensitive than any other instruments of its kind (Paik, 1996). This instrument was used to perform a test of the inverse-square law of gravity at a level of sensitivity 10 times beyond that of the other methods at laboratory distance scales (Moody and Paik, 1993). The device proposed here has strong similarities to the existing instrument; however, by reducing the resonance frequency of the accelerometer and performing a *resonance* experiment, the amplifier noise contribution is made negligible and the acceleration sensitivity is greatly enhanced.

The main challenge of the new experiment is construction of a spin source that can be modulated to near saturation at the signal frequency of 0.01 Hz. Over the past two years, we have concentrated on constructing a suitable spin source for our ground experiment. We have now fabricated and tested a spin source with alternating sections of ferromagnetic material (Magnifer 7904 from Ed Fagan, Inc., Franklin Lakes, NJ) and copper (Cu). In this paper, we report the design and performance of this spin source.

2. Design of the Spin Source

Figure 1 is a cross sectional view of the experiment. Two superconducting angular test masses are suspended by magnetic levitation around a common spin source of toroidal geometry. Each test mass is composed of 16 vertical ridges formed inside a cylindrical shell of niobium (Nb). The ridges of the two test masses are aligned with respect to the spin source such that the test masses are driven differentially by the single spin source.

For an electron with its spin polarized in the direction $\hat{\mathbf{S}}$ and an unpolarized nucleon, the interaction potential is given by (Moody and Wilczek, 1984):

$$V_a = g_s g_p \frac{\hbar^2}{8\pi m_e} (\hat{\mathbf{S}} \cdot \hat{\mathbf{r}}) \left(\frac{1}{r} + \frac{1}{r^2} \right) e^{-r/l}, \quad (1)$$

where g_s and g_p are dimensionless coupling constants, m_e is the mass of the electron, $\hat{\mathbf{r}}$ is the unit position vector of the nucleon relative to the electron, and l is the range of the force, which is inversely proportional to the axion mass. This interaction potential gives rise to an identically vanishing torque for any closed loop of spin (Shaul *et al.*, 1996). Thus, a source with alternating materials is needed, with the greatest possible contrast between the spin densities of the two materials desired.

For transition-metals, crystal field quenching of orbital angular momentum implies that total atomic angular momentum approximately equals the intrinsic spin. At temperatures much less than the Curie temperature, the spin density \mathbf{r}_s is given by

$$\mathbf{r}_s = \frac{\mathbf{M}}{g \mathbf{m}_b}, \quad (2)$$

where \mathbf{M} is the magnetization, g is the spectroscopic splitting factor (≈ 2), and \mathbf{m}_b is the Bohr magneton. Hence, materials with similar saturation magnetizations will have similar maximum spin densities. On the other hand, having a large difference between the saturation magnetization of the two materials will cause unacceptably large stray fields.

The solution may lie in the use of materials containing rare-earth elements. In many of these, the orbital angular momentum component of the total angular momentum, which does not contribute to the spin-mass coupling force, is very large. The rare-earth elements below gadolinium (Gd)

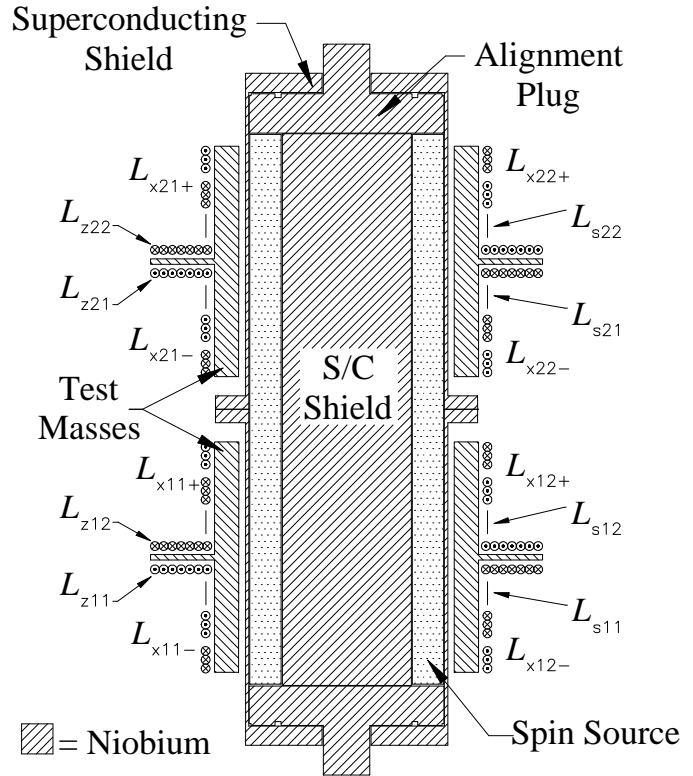


Figure 1. Cross sectional view of the experiment

are particularly interesting, because for these the intrinsic spins are anti-parallel to the magnetization. Unfortunately, rare-earth materials tend to be hard ferromagnets, which, for a cryogenic experiment, generate an intolerably large amount of heat upon spin modulation.

We have therefore chosen a source design that combines a soft transition-metal ferromagnet (Magnifer 7904: 80% Ni, 14% Fe, 5% Mo) with a non-magnetic material (Cu). In this design, since $m_{\text{mag}} \gg m_0$, the magnetic induction B , and hence $M (= B/m_0)$ in the Magnifer, will be limited by the ability to shield the B field in the regions of Cu. Because of this limitation, the achievable magnetization will not approach the saturation value. Therefore, to limit the heat dissipation, we have chosen a very *soft* ferromagnet as opposed to one with a high maximum spin density.

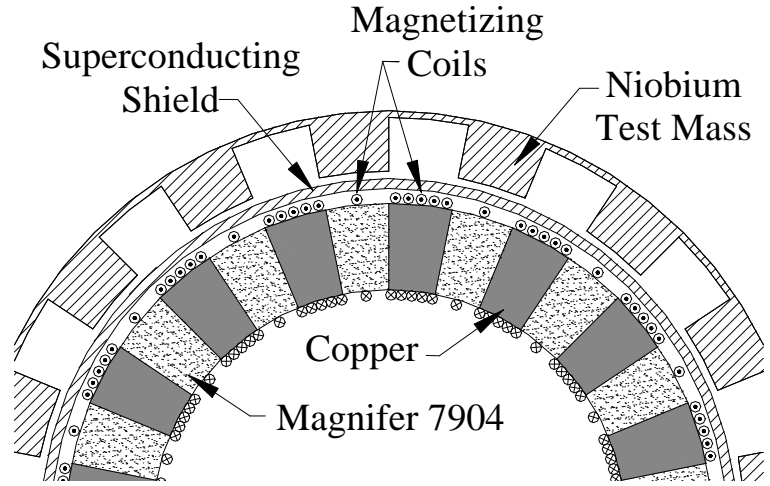


Figure 2. Cross sectional view of the test mass and the spin source

Figure 2 shows a cross section of the test mass and the spin source. The source is a cylindrical shell (or a toroid) with an outer radius 2 mm less than the inner radius of the test masses, a thickness of 5 mm and a length of 107 mm. It is composed of 32 alternating strips of Magnifer and Cu. Two single-layer niobium-titanium (NbTi) coils are wound about the respective materials to provide and monitor the magnetizing field. A 0.25 mm thick Nb sheet shields the test masses from the magnetic field in the spin source. The field generated by the coil on Cu is absorbed into the high-permeability region of Magnifer, thus staying within the toroid. The field generated by the coil on Magnifer, however, tends to wrap around each section of Magnifer. In our design, this is prevented by wrapping the source toroid tightly with a Nb shield.

3. Construction and Test of the Spin Source

In order to construct the spin source, 32 alternating strips of the spin source, 16 each respectively from Magnifer and Cu, were machined with a wire EDM (electron discharge machine). The Magnifer was heat-treated in a high vacuum oven at 1070°C for 5 hours to obtain a high m . The Magnifer and Cu strips were then diffusion-bonded at 670°C for 12 hours in the oven to form a toroid, the desired source geometry. After machining the source to its final shape with required grooves and holes, sharp corners were filed individually in preparation for coil winding.

Winding single-layer toroidal coils over the spin source was a pains-taking process. A NbTi wire of 0.15 mm diameter (including insulation) was used to wind the coils. The maximum number of turns that could be wound over each section of Cu was 17, which allowed a total of 272 turns for the magnetizing coil wound over Cu. A smaller, 16-turn coil was wound over Magnifer, 1 turn over each section. The computed self-inductances of these coils, including known stray inductance, were $L_{\text{Cu}} = 952 \mu\text{H}$ and $L_{\text{Mag}} = 4.3 \mu\text{H}$, respectively. With this design, a

current of 20 A in the magnetizing coil is expected to generate a B field of 0.13 T through the toroid. After winding the coil, the source was wrapped with a Nb shield by using a specially designed aluminum structure which holds sections of 0.25-mm thick Nb sheet all around the source. Figure 3 is a photograph of the spin source before it was assembled with the shield and the support structure.



Figure 3. Photograph of the spin source

The spin source was then cooled to 4.2 K to verify its magnetization characteristics. The most important parameters we needed to verify were the self-inductances of the two coils, L_{Cu} and L_{Mag} , the coupling constant k^2 between L_{Cu} and L_{Mag} , and the maximum current, I_{max} , we can send through L_{Cu} . These can be combined to determine the maximum magnetization, M_{max} , achievable in the Magnifer. A near-unity coupling would indicate that the superconducting shield indeed forces the magnetic field to go around the entire toroid without generating significant stray fields around each section of Magnifer. The value of M_{max} would yield the maximum spin signal that we can use for our spin-mass experiment. The achievable magnetization could be limited by the critical current of one of the many superconducting joints in the magnetizing coil or by the stray magnetic field from the coil exceeding the critical field of the Nb shield.

The self and mutual inductances of the coils, as well as their effective series resistances, were measured as functions of frequency $f = \omega/2\pi$. A four-point measurement technique was used to eliminate the effect of lead impedance. At $f \geq 10$ Hz, the inductances and resistances exhibited frequency dependence of $\sim \omega^{-1/2}$ and $\sim \omega^{1/2}$, respectively. This was expected from the effect of skin depth $d = (2/\mu\sigma\omega)^{1/2}$, where σ is the conductivity of the material. For Cu at 4.2 K, d becomes comparable to the dimensions of the material, ~ 5 mm, at f between 1 and 10 Hz. Above this frequency, the relevant volume for L and R is reduced as $\omega^{-1/2}$, resulting in the observed frequency dependence. The skin-depth effect drops rapidly at $f < 1$ Hz, indicating that d is significantly greater than the thickness of the source at these frequencies. In this frequency range, all losses due to eddy currents occur in the Cu, since σ is much greater for Cu than for Magnifer.

The measured values of the inductances at $f = 0.03$ Hz are

$$L_{Cu} = 943 \mu\text{H}, L_{Mag} = 6.54 \mu\text{H}, \text{ and } M = 57.8 \mu\text{H}. \quad (3)$$

This yields $k^2 = 0.54$. Notice that L_{Cu} agrees closely with its computed value, 952 μH . However, L_{Mag} is 50 % higher than its expected value, 4.3 μH . This increased inductance may be due to the fact that the Nb shield cannot completely prevent the field from wrapping around the single turn

of wire wound on each section of Magnifer. Such a field would increase L_{Mag} and reduce k^2 . The close agreement of the measured L_{Cu} with the computed value confirms that our theoretical model for the spin source is basically correct and the B field from L_{Cu} indeed feeds though the entire toroid, aligning the electron spins in Magnifer.

The maximum current I_{max} used during the measurements was limited to an amplitude of 13 A. This value was limited by heating of the resistor used to monitor the current. This resistor will not be used during the experiment; however, to stay below the critical field (H_{c1}) of the Nb shield, we will limit I_{max} to 20 A. This gives $M_{\text{max}} = 7.3 \times 10^4$ A/m rms and a spin density of $3.9 \times 10^{21} \text{ cm}^{-3}$. This corresponds to 17 % of the maximum spin saturation in Magnifer. Spot-welded superconducting joints made for the wire have been shown to carry over 20 A.

The measured effective resistance (in series) at 0.03 Hz is $2 \times 10^{-6} \Omega$. At the 20-A amplitude, this resistance will result in a power dissipation of 400 μW . Adequately heat sinking the source to the helium bath should minimize any heating due to this dissipation. Also, any residual temperature effects would appear at harmonics of the signal frequency, which can be filtered out.

4. Conclusions

A spin source for use in a spin-mass coupling experiment has been fabricated and tested. The design combines alternating regions of a soft, high-permeability material, Magnifer, and a non-magnetic material, Cu. This source will give reasonably high spin density while maintaining low power dissipation. A spin density of $4 \times 10^{21} \text{ cm}^{-3}$ can be reached while staying below the critical field of the superconducting shield. Power dissipation due to hysteresis is negligible for the magnetically soft Magnifer, while eddy current losses in the Cu are manageable. Combining this source with extremely sensitive angular accelerometers will allow a spin-mass coupling experiment with sensitivity several orders of magnitude beyond that of previous experiments.

With the spin source successfully completed and our theoretical model confirmed, we are now ready to construct the rest of the apparatus. Over next several months, we will construct the superconducting differential angular accelerometer and assemble the entire apparatus for the spin-mass coupling experiment.

References

- Moody, M. V. and Paik, H. J. (1993), *Phys. Rev. Lett.* **70**, 1195.
- Moody, J. E. and Wilczek, F. (1984), *Phys. Rev. D* **30**, 130.
- Paik, H. J. (1996), in *SQUID Sensors: Fundamentals, Fabrication and Applications*, ed. H. Weinstock (Kluwer, Dordrecht), p.569.
- Paik, H. J., Canavan, E. R., and Moody, M. V. (1999), in *Proceedings of the Eighth Marcel Grossmann Meeting on General Relativity*, ed. T. Piran (World Scientific, Singapore), p. 1197.
- Peccei, R. D. and Quinn, H. (1977), *Phys. Rev. Lett.* **38**, 1440.
- Shaul, D. *et al.* (1996), *Class. Quantum Grav.* **13**, A107.
- Weinberg, S. (1978), *Phys. Rev. Lett.* **40**, 223.
- Wilczek, F. (1978), *Phys. Rev. Lett.* **40**, 279.

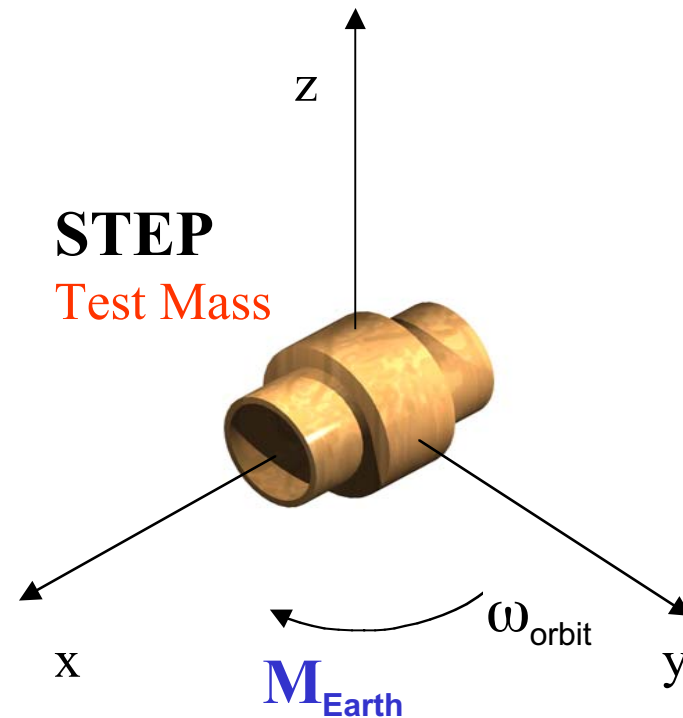
Satellite Test of the Equivalence Principle

STEP NOISE SOURCES

- **Environment Stability**
 - Thermal Stability
 - Mechanical Stability (Platform Stability and Residual Pressure)
- **Forces Acting on Test Masses**
 - **Gravitational Forces**
 - **Test Mass Shape**
 - Electromagnetic Forces
 - Shield Magnetic Forces
 - Control Charge on Test Masses (and Surfaces Near Masses)
 - Mechanical Forces
 - Vibration of Platform
 - Residual Vapor Pressure
 - Impact of Particles from South Atlantic Anomaly

STEP Science Instrument ACCELEROMETER ORIENTATION

- Test Mass Center Of Mass
Coordinate System Origin
- Earth Center Of Mass
X-Y Orbit Plane
- Accelerometer Signal Axis
X-Axis
- Signal Frequency
Orbit Frequency ω_{orbit}
 \pm Z-Axis Roll Rate ω_{roll}



STEP Science Instrument TEST MASS SHAPE

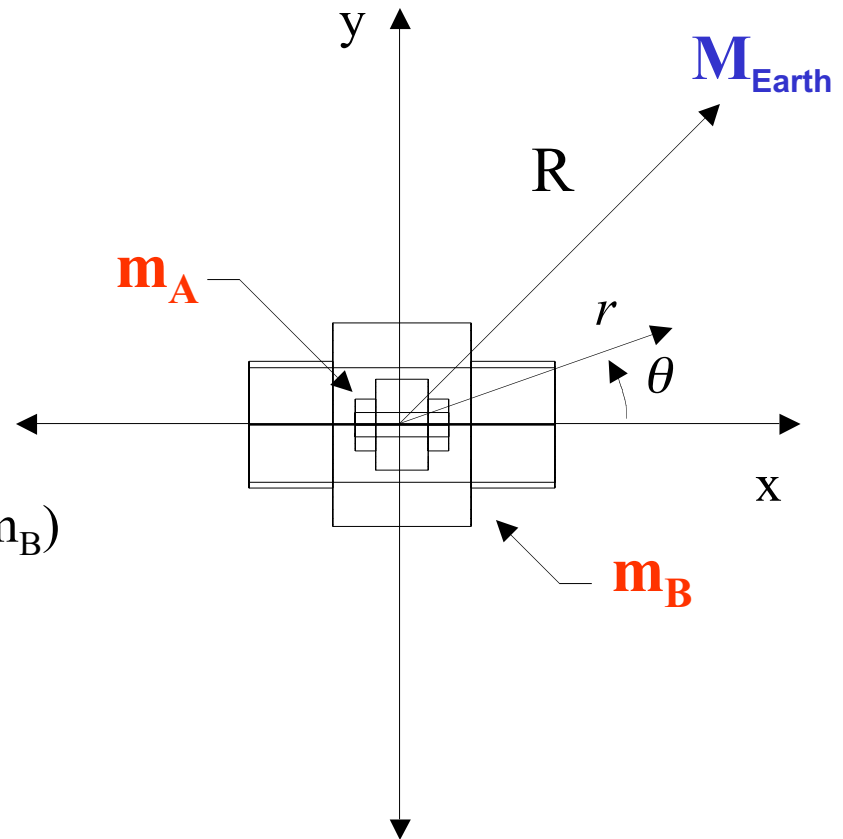
- *IDEAL* EP Test

$$\frac{\phi_A^{Earth}}{m_A} = \frac{\phi_B^{Earth}}{m_B}$$

- *COINCIDENT* Mass Centers
- *EQUAL* Mass Moments ($m_A = m_B$)

- Belted Cylinder Shape

- *ALIGN* Mass Centers
- *MATCH* Mass Moments



STEP Test Mass

GRAVITATIONAL POTENTIAL*

- Mass $\mathbf{m_A}$ Source Field $\mathbf{M_S}$

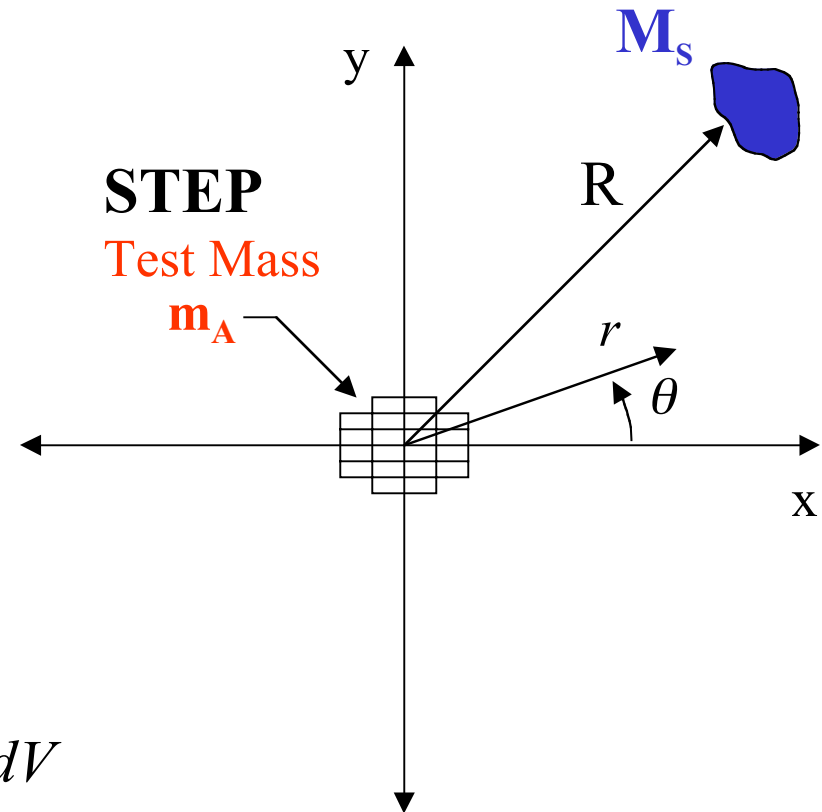
$$\phi_A^S = -4\pi G \sum_{n=0}^{\infty} \frac{1}{2n+1} \sum_{m=-n}^{m=n} q_{nm}^A Q_{nm}^S$$

- $\mathbf{q_{nm}}$ Multipole **Mass Moment**

$$q_{nm}^A = \int_{\text{Volume } m_A} \rho_A(r, \theta, \varphi) r^n Y_{nm}^*(\theta, \varphi) dV$$

- $\mathbf{Q_{nm}}$ Multipole **Source Field**

$$Q_{nm}^S = \int_{\text{Volume } M_S} \rho_S(r, \theta, \varphi) r^{-(n+1)} Y_{nm}(\theta, \varphi) dV$$



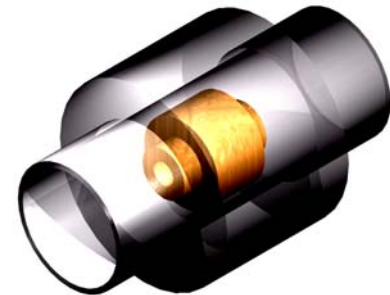
*Y. Su, B. Heckel, E. Adelberger, J. Gundlach, M. Harris, G. Smith, and H. Swanson, Phys. Rev. D 50, 3614 (1994)

STEP Test Mass

MATCHING MASS MULTIPOLE MOMENT*

$\times 10^6$					
n	2	4	6	8	10
$\frac{q_{n0}^A}{m_A}$	0.025	0.005	0.031	-0.001	0.000
$\frac{q_{n0}^B}{m_B}$	-0.034	-0.009	0.028	-4.250	-0.450
$\left \frac{q_{n0}^A}{m_A} - \frac{q_{n0}^B}{m_B} \right $	0.059	0.014	0.003	4.249	0.450

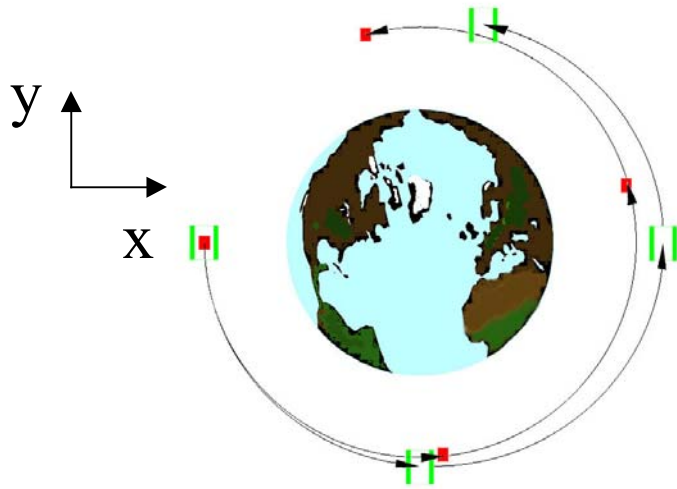
• $n = 8$



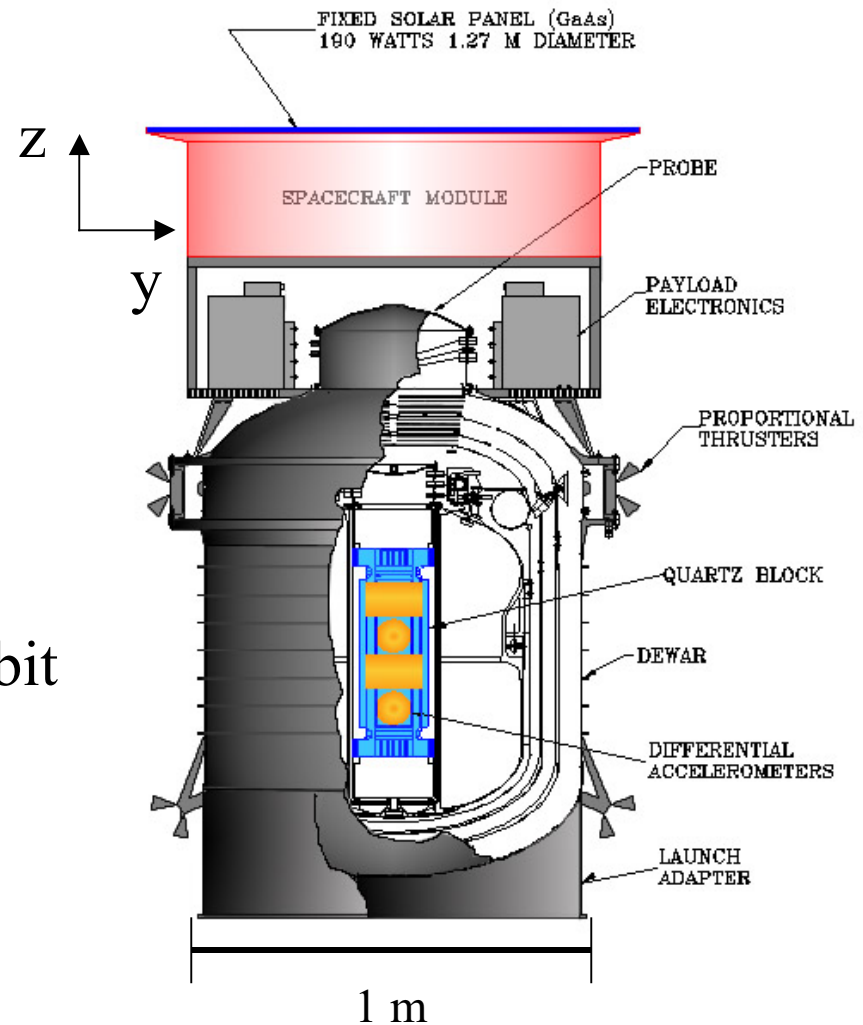
*N.A. Lockerbie, X.Xu, and A.V. Veryaskin, Class. Quantum Grav. 11, 1575 (1994)

STEP Spacecraft

SERVICE MODULE AND PAYLOAD



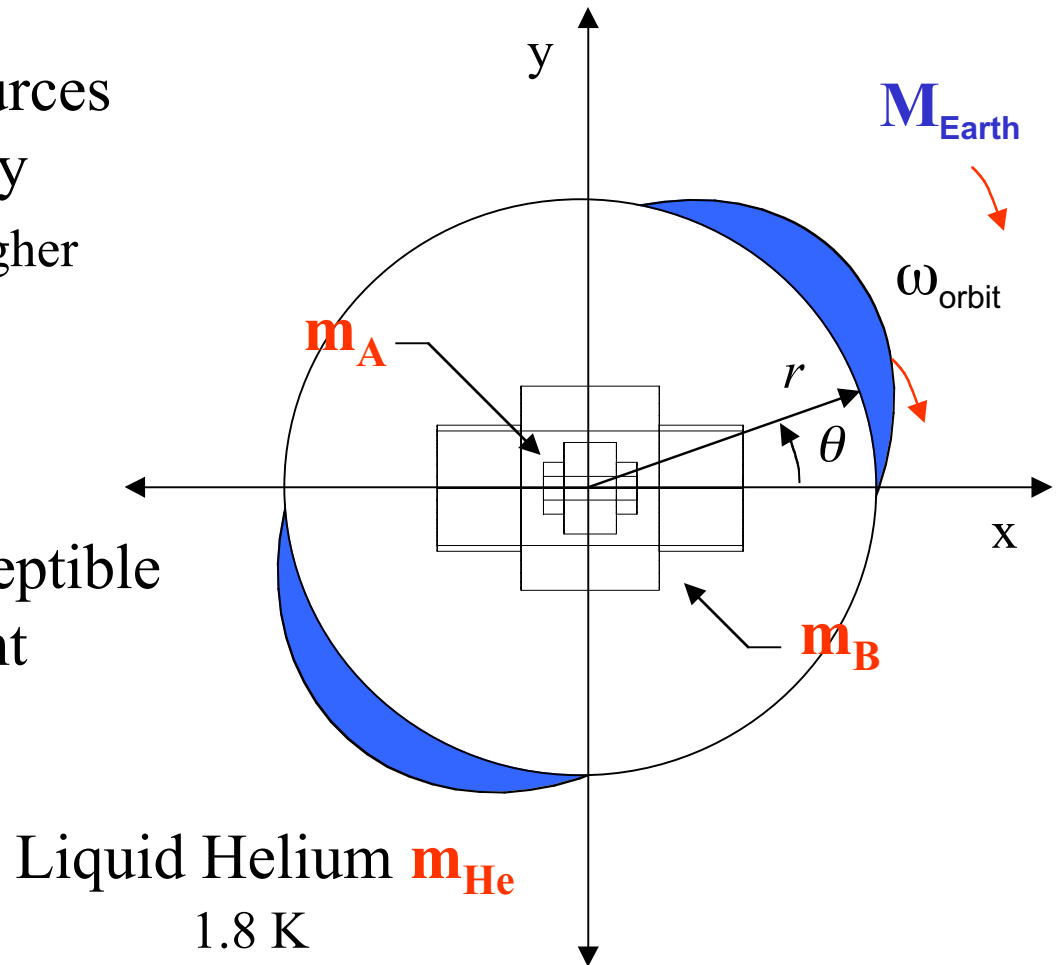
- Sun Synchronous Polar Orbit
 - 400 - 500 km
 - 97 Degree Inclination



Liquid Helium Motion

HELIUM TIDE

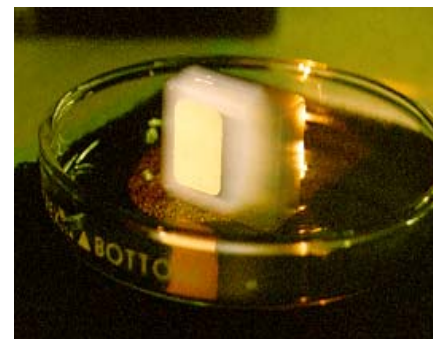
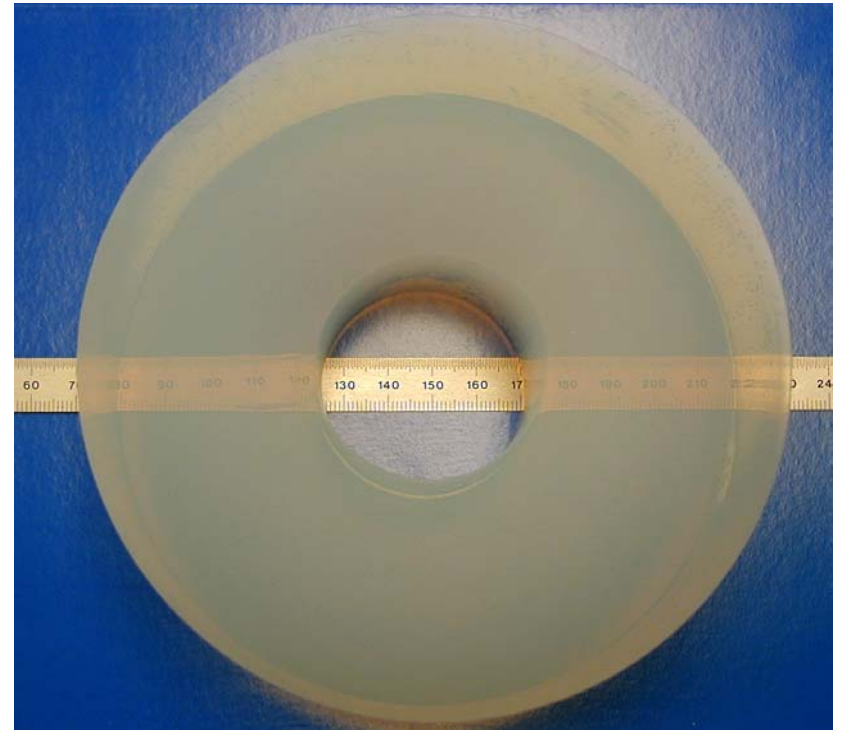
- Nearby Gravitational Sources Act on Masses Differently
 - Imperfect Matching of Higher Mass Moments ($n = 8$)
 - Differential Acceleration
- Liquid Helium m_{He} Susceptible to **Earth** Gravity Gradient
 - Signal Bandwidth



Ultra-lightweight Porous Material

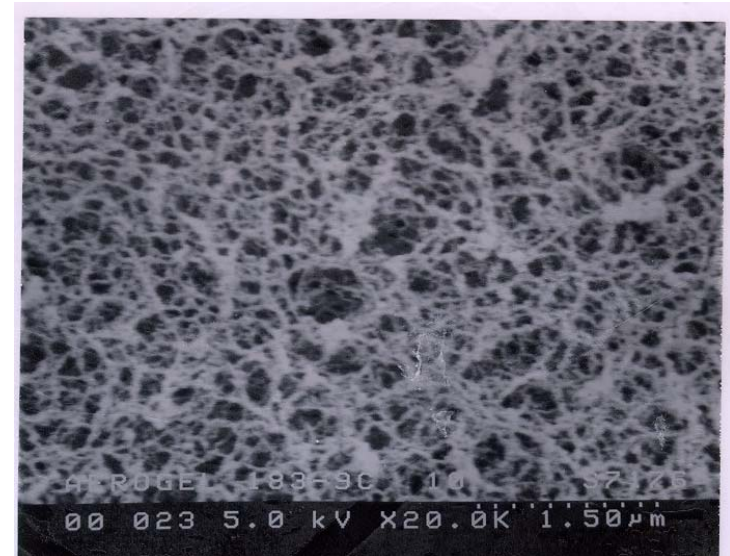
SILICA AEROGEL

- Silica aerogel is a highly porous silica glass
 - Porosity as high as 99 %
leading to densities as small as **0.02** g cm⁻³ (20 kg m⁻³)
- Silica aerogel can be machined, coated with metallic films, manufactured with embedded elements...



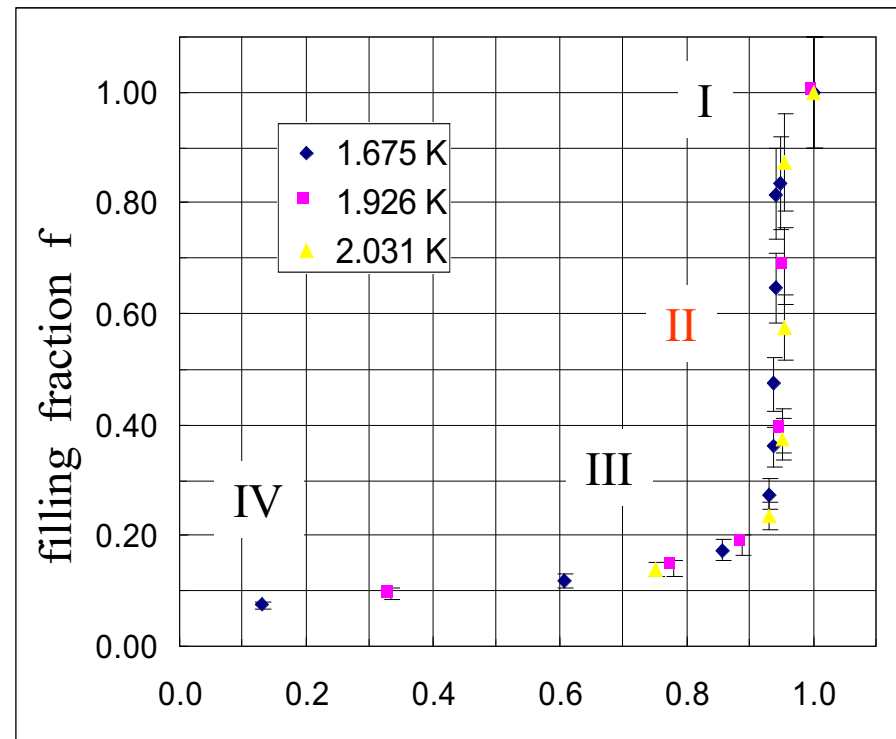
Silica Aerogel SEM Image

- Fundamental building blocks are **2 nm diameter silica spheres** shown in white
- SEM studies show a large range of void sizes with the majority of the void volume consisting of void sizes 100 to 1000 nm



Silica Aerogel Adsorption Isotherm

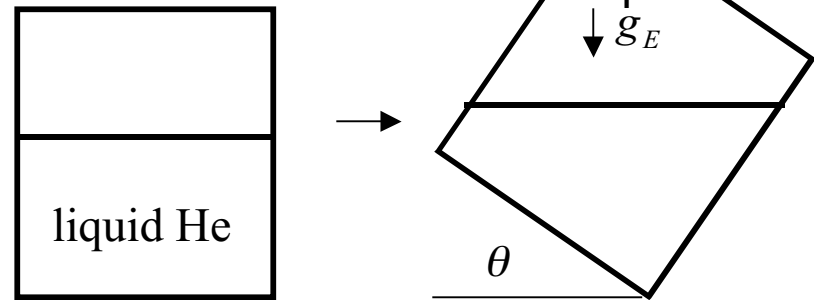
- Type I: silica aerogel filled with helium $f = 1$
- Type II: macroscopic voids 100 to 1000 nm
- Type III: mesoscopic voids 10 to 100 nm
- Type IV: helium film on silica aerogel



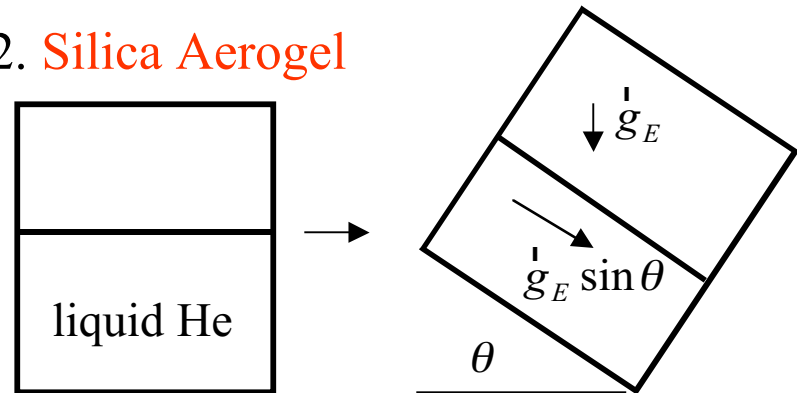
Silica Aerogel Experiment I

- Observe response of the liquid helium surface in silica aerogel to changes of order 0.1 g_E across 2 cm (0.02 m)
- No shape change implies no shape change for 10^{-6} g_E across 100 cm (1 m)

1. No Silica Aerogel

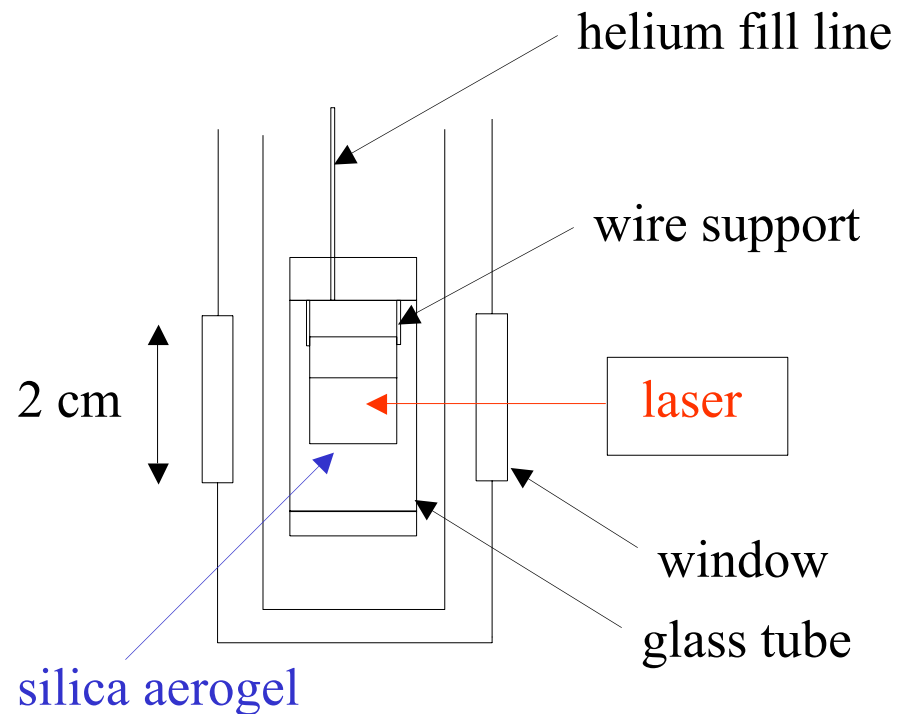


2. Silica Aerogel



Silica Aerogel Experiment I*

- Silica aerogel is transparent
- Use cryogenic system with optical access to observe surface of liquid helium
- Silica aerogel in sealed glass cell in liquid helium bath at constant temperature

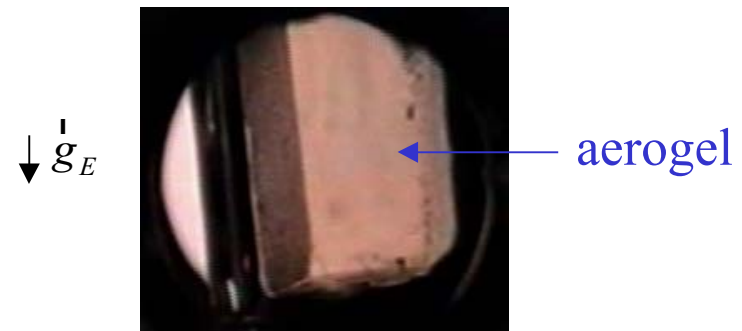


*R. Dolesi, F. Rossi, R. Torii, and S. Vitale, COSPAR Proceedings, Nagoya, Japan (1999)

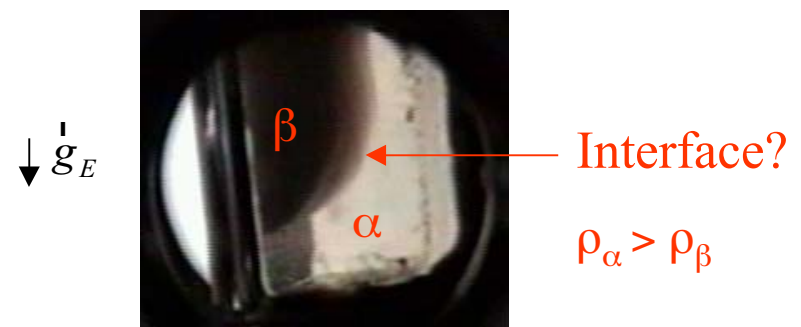
Silica Aerogel Experiment I

- Observe dark spots due to light scattering by vapor voids (also seen for liquid nitrogen in aerogel by Chan et al.*)
- Dark β regions of lower density than transparent α regions
- Tilting cell had no effect on the shape of the interface

1. No Liquid Helium

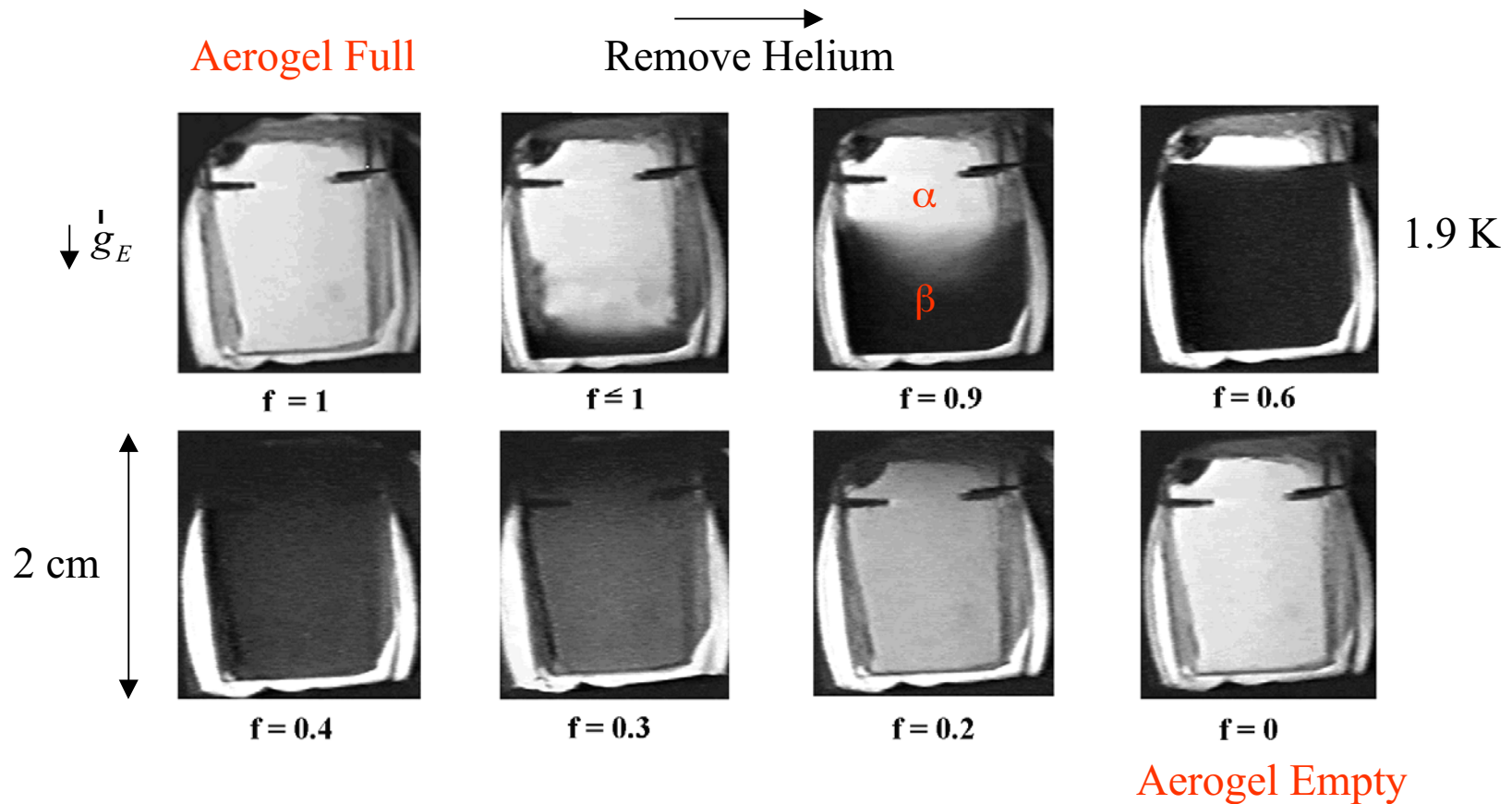


2. Liquid Helium in Aerogel



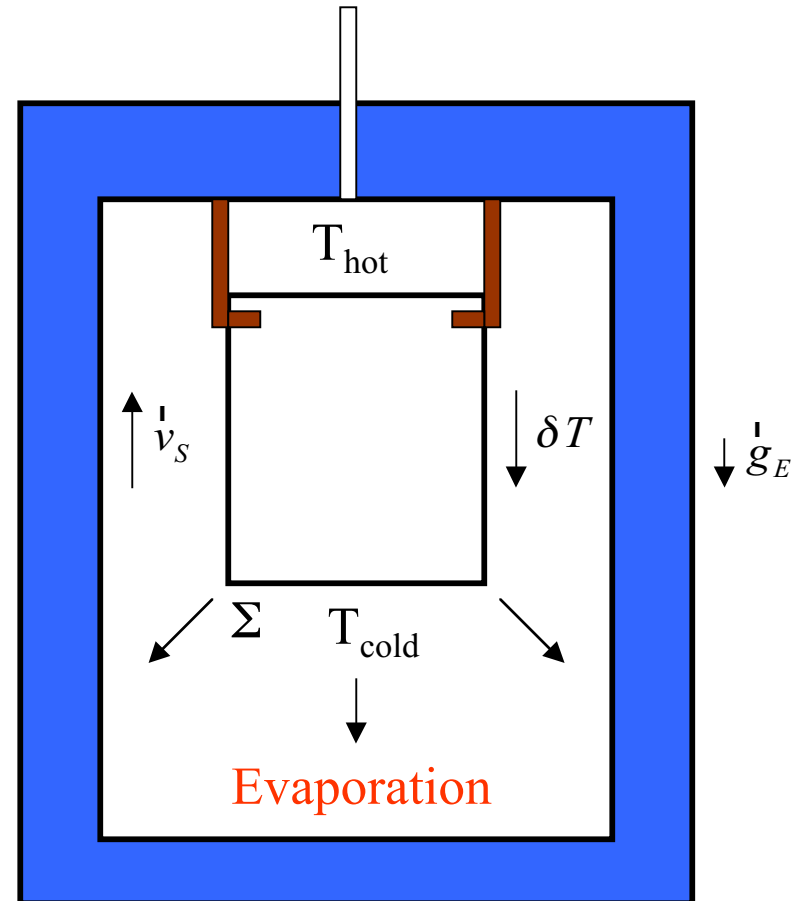
*A. Wong, S. Kim, W. Goldburg, and M. Chan, Phys. Rev. Lett. 70, 954 (1993)

Removing Superfluid Helium from Aerogel



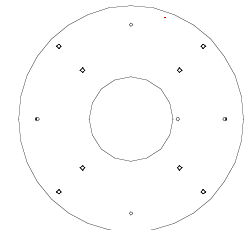
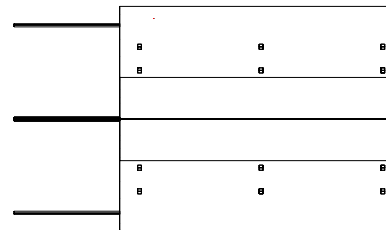
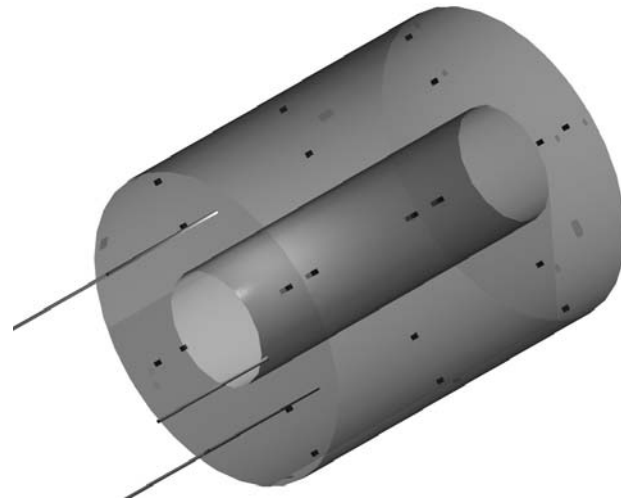
Thermal Gradient Model

- Liquid helium is removed near surface of aerogel by **evaporation**
- **Thermal link** to cell at temperature T_{hot} produces thermal gradient δT
- Thermal gradient produces mechanical force on liquid helium by thermomechanical “fountain effect”



Large-Scale Aerogel Experiment

- Cast aerogel in 2 liter container
- Fill aerogel with superfluid helium
 - adsorption isotherm $P(f)$
 - temperature distribution $T(x,y,z)$
- Shake test aerogel filled with superfluid helium



SETTING NEW BOUNDS ON THE SIZE OF ANOMALOUS SHORT RANGE FORCES

S. Wang and J. A. Lipa

Physics Department, Stanford University, Stanford, CA. 94305

About 12 years ago, some evidence began appearing that indicated a possible deviation from Newtonian gravity on terrestrial length scales in both new and old experiments. It was hypothesized that a new force similar to gravity might exist, but scaling differently with the spacing of the interacting bodies. So far, no positive result has been verified. The work described here is a continuation of this search concentrating on small length scales, where the limits set to date are very weak. This work is motivated by a new analysis of supersymmetry-breaking particle theories that predicts the existence of such a force in many plausible scenarios. Improving the limit on the possible strength of the force at short ranges would aid in the elimination of a number of these theories. The new predictions are for Yukawa-type forces with strengths spanning the range from 10^5 to 10^{-1} times gravity, acting over corresponding length scales of 10^{-5} to 3×10^{-3} m. Current experimental limits are up to 5 orders of magnitude higher. Our measurements have substantially improved this limit on length scales below 10^{-4} m. Our approach was based on detecting the frequency shift of a high-Q mechanical oscillator due to the excess spring constant of the new force, as a function of the separation of two small masses. Longer term, it appears possible to resolve down to 30 - 100 times gravity with this technique.

INTRODUCTION

In the mid '80s it became apparent that there were some small but possibly significant inconsistencies between various gravitational experiments performed on earth. It appeared that high resolution experiments were beginning to detect small deviations from Newton's law of gravitation. This gave impetus to a new round of work and additional reviews of old data, with the intent of detecting or setting new limits on a hypothetical force similar to gravity, but scaling differently with the spacing of the interacting bodies. So far, no positive result has been verified, and the most careful, well designed experiments give a null result. One difficulty has been the lack of a credible mechanism to generate such a force, although a number of theoretical models were developed, and in recent times research in this area has waned. Recently a new analysis of supersymmetry-breaking particle theories has predicted the existence of such a force in some interesting scenarios. Improving the limit on the possible strength of the force would aid in the elimination of a number of these theories. The new predictions are for Yukawa-type forces with strengths spanning the range from 10^5 to 10^{-1} times gravity, acting over corresponding length scales of 10^{-5} to 3×10^{-3} m. Current experimental limits are up to 5 orders of magnitude higher. The ground-based experiment described here substantially improves this limit on length scales below 10^{-4} m. Our approach is based on detecting the frequency shift of a high-Q mechanical oscillator due to the excess spring constant of the new force, as a function of the separation of two small masses, one attached to the oscillator.

Experiments searching for anomalous forces fall into two categories. One consists of searching for departures from the inverse square law, and the other consists of searching for a composition-dependent force. The two are related in that a force coupled to hypercharge might manifest itself to first order as an intermediate range correction to gravity. Substantial work has been done on searching for an intermediate to long range anomalous force. This work has been summarized by Fischbach et al.¹. So far, no conclusive positive evidence has been found. In 1985 Hoskins et al.² performed an elegant laboratory experiment to look for possible deviations from the inverse square law in the range from 2 to 105 cm. This experiment currently sets the upper limit on a possible Yukawa type of force in the centimeter range. For smaller force ranges, this constraint rapidly becomes less stringent. Using a well

designed spring balance and capacitive position detection technique, Sparnaay³ measured the Casimir force between two parallel metal plates with a separation distance of 0.5 μm to 2 μm . From the force magnitude measured, an upper limit on the existence of the Yukawa type of force can be estimated. This limit is less than 10^{10} g for a force range of 0.1 mm. This experiment currently sets the limit for very short length scales. Recently Carugno, et al.⁴ improved the limit near 10^{-4} m by two orders of magnitude using a cantilever oscillator. With spherical masses and torsion balance technique, Mitrofanov and Ponomareva⁵ placed a tight bound on the force over the range 2×10^{-3} to 10^{-4} m. Figure 1 shows these limits as a function of range.

Israelachvili and Tabor⁶ (IT) used a frequency shift method to measure the van der Waals force between two plates as a function of distance between them in the range of 10 to 130 nm. There the detection mass was elastically supported by a piezoelectric bimorph strip which served both as a spring and a detection device. The distance of the driving mass to the detection mass could be changed by means of a micrometer for coarse adjustment and by a piezoelectric transducer for fine control. The piezoelectric transducer was also used to excite the driving mass into small amplitude oscillation to couple to the detection mass. Although the detection mass assembly had a Q of only 50, the authors could resolve a resonant frequency change of 1 part in 10^6 . Unfortunately, it is hard to recast this experiment in terms of an inverse square law test, as critical dimensions were not given in the paper. However, its sensitivity was probably comparable to Sparnaay's experiment.

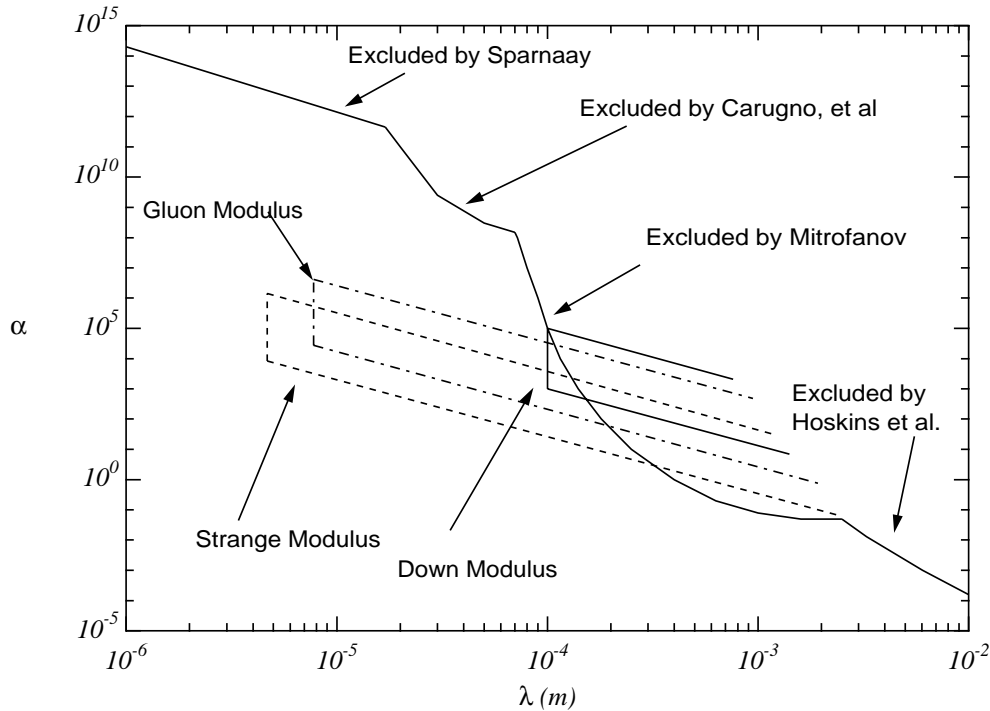


Figure 1: Comparison of existing detection limits with predicted force strengths, α , as a function of Yukawa range, λ . (See ref. 7)

Dimopoulos and Giudice⁷ (DG) have discussed the possible existence of an anomalous force in the context of superstring theory. This is very important because superstring theory holds the promise of

unifying the forces of nature. Yet so far, there is no evidence to guide these theories beyond the requirement for consistency with known physics. The positive or negative verification of a prediction in this area would go a long way to establishing the direction of future theoretical work. A trademark of superstring theories is the occurrence of gravitationally coupled massless scalars called moduli. To avoid conflict with Newtonian gravity, moduli must obtain mass. One possibility is that stringy non-perturbative phenomena create a potential which gives them a mass. A second possibility is that Planckian physics leave the moduli massless and they obtain mass only as a result of supersymmetry breaking. Theories with low energy supersymmetry breaking are of interest because of their applicability to supersymmetry flavor problems. Moduli in these theories are so light that they can have macroscopic Compton wavelengths and mediate macroscopic forces of gravitational strength. Based on the calculations of DG, the range of such forces could be on the scale of 10^{-5} to 3×10^{-3} m and the strength could be from 10^5 to 10^{-1} times gravity. In figure 1 we also show the predicted strengths as a function of range and compare them with the current experimental limits. It can be seen that there is a large region of parameter space still allowed, in which theoretical predictions exist.

APPARATUS

The experiment builds on the resonance technique of IT, extending it to the case of gravitational effects at longer ranges. The basic approach was to look for a frequency shift of a small mechanical oscillator due to the additional spring constant associated with an anomalous force gradient. Since this shift is affected by the existing spring constants, it is desirable to operate the oscillator with the lowest spring constant and highest Q. Basically one must maximize frequency discrimination and ensure the stability of the resonant frequency. Our initial design approach was to fabricate a simple torsional oscillator with a dense supported mass near a high density movable plate. The movable plate can be adjusted by a translation stage controlled hydraulically. The spacing between the source mass and test mass is measured capacitively. A schematic view of the apparatus is shown in figure 2. Magnetic forces were reduced by selecting highly non-magnetic materials recommended for use on the GP-B program. These materials have been scanned with a sensitive SQUID-based magnetic gradiometer and their magnetic signatures are well documented. The excitation and readout of the oscillator frequency were by capacitive techniques, using a small electrode attached to the body of the vibration isolator. The resonant frequency was determined by using a phase-locked loop and data were logged by a Macintosh running Labview software.

It was necessary to pay careful attention to potential sources of spurious effects that might mimic a non-gravitational signal. Provision was made for a ground plane between the masses to attenuate electrostatic and Casimir effects substantially, if a signal was detected. As noted earlier, IT claims a frequency discrimination capability of a part in 10^6 with a Q of 50 at around 100 Hz. This corresponds to splitting the resonance line to about a part in 20,000, which is conservative today, using digital signal processing techniques and modern low-noise amplifiers. However, in our experiments to date, we have only split the resonance line to a part in 10^3 due to the existence of thermal drifts. By paying careful attention to loss mechanisms and operating at temperatures around 77 K, we expect to be able to achieve

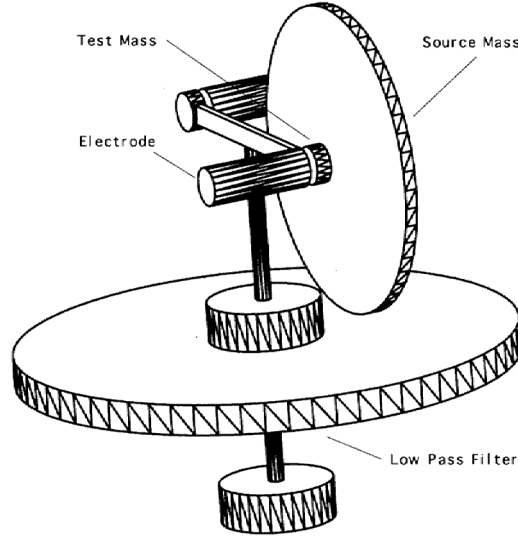


Figure 2: Schematic view of the apparatus.

Q's of at least 3000 and substantially reduce thermal effects. We note that at room temperature mechanical Q's of 3×10^7 have been achieved in large silicon resonators⁸, and 50,000 in small quartz cantilever systems used for atomic force microscopy⁹.

In the remainder of this section we give some estimates for the quantities of interest in the experiment. A rough idea of the sensitivity of such a system can be obtained as follows: Following Price¹⁰, it is easy to show that the force between two parallel plates due to a Yukawa interaction is

$$F_Y(d) = 2\pi\alpha G\rho_1\rho_2 A\lambda^2 \exp(-d/\lambda)[1 - \exp(-t_1/\lambda)][1 - \exp(-t_2/\lambda)] \quad (1)$$

where d is the distance between the facing surfaces of the plates, α and λ the strength and range parameters of the Yukawa-like potential, ρ and t the density and thickness of the plates, and A the area of plate 1. The surface area of plate 2 is assumed to be infinite. For small vibration amplitudes, we take $d = d_0 + d'$, where d_0 is the equilibrium distance and d' a small deviation from it during vibration. For $d' \ll \lambda$, we can expand the right hand side of eq. (1) and the term linear in d' is

$$F_Y(d') = -2\pi\alpha G\rho_1\rho_2 A\lambda \exp(-d_0/\lambda)[1 - \exp(-t_1/\lambda)][1 - \exp(-t_2/\lambda)] d'$$

Thus the equivalent additional spring constant due to the Yukawa-type force is

$$k_Y = \frac{\partial F_Y(d')}{\partial d'} = -2\pi\alpha G\rho_1\rho_2 A\lambda \exp(-d_0/\lambda)[1 - \exp(-t_1/\lambda)][1 - \exp(-t_2/\lambda)] \quad (2)$$

The frequency shift due to the existence of the 5th force would be

$$\Delta f = (1/2\pi) [(k/m_e + k_Y/m_1)^{1/2} - (k/m_e)^{1/2}] \quad (3)$$

where k is the effective spring constant of the cantilever, and m_1 and m_e are the mass and effective mass of plate 1, respectively. As an example, for a system with a resonant frequency of 15 Hz and with $m_1 = 1.2$ gm, $d_0 = 0.06$ mm and $\lambda = 0.1$ mm, we estimate a frequency shift of 1 μ Hz for $\alpha = 5 \times 10^4$.

RESULTS

A number of runs have been performed with the apparatus. Initially the testing concentrated on obtaining a high Q in the mechanical oscillator. So far we have attained a Q of 1500 at room temperature with a beryllium-copper torsional oscillator operating near 145 Hz. The predominant change in frequency is caused by the change of room temperature. A thermistor was attached to the oscillator isolation stage and the temperature dependence of the frequency was measured. All frequencies measured were then corrected for temperature. The measurement is performed by alternating the source-to-test-mass gap between 0.1 mm and 2 mm at intervals of 20 minutes. The frequency is averaged over this period for each gap and the difference taken between the two frequencies. In figure 3 we show a histogram for a collection of 1590 samples of these frequency differences. The solid line in the figure is a Gaussian fit. Based on the mean value of the histogram we derive from eqs. 2 and 3 the limit set by our experimental data on the anomalous force amplitude and range as shown in figure 4.

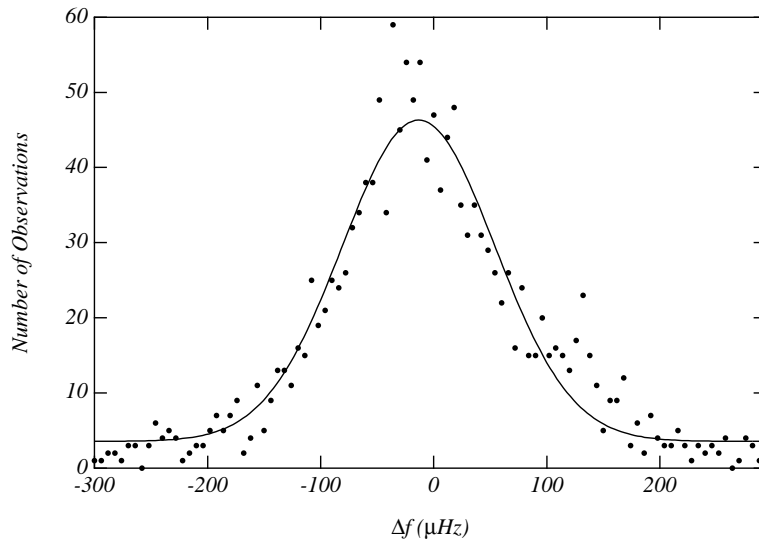


Figure 3: Histogram of frequency shift data with Gaussian fit.

CONCLUSIONS

To date we have been able to lower the bound set by Carugno et al⁴ by over an order of magnitude. While this is a substantial improvement, much more needs to be done before the supersymmetry predictions are impacted significantly. From eqs. 2 and 3 it can be seen that the frequency shift increases with decreasing k and increasing ρ_1 and ρ_2 . This is just another way of saying that the best resolution is obtained with the weakest supporting spring constant and heaviest masses, as might have been guessed intuitively. Thus one is quickly driven to vertical support systems with attendant pendulation problems. For a stable, high Q oscillator operating at 1 Hz with $\lambda = 0.3$ mm and

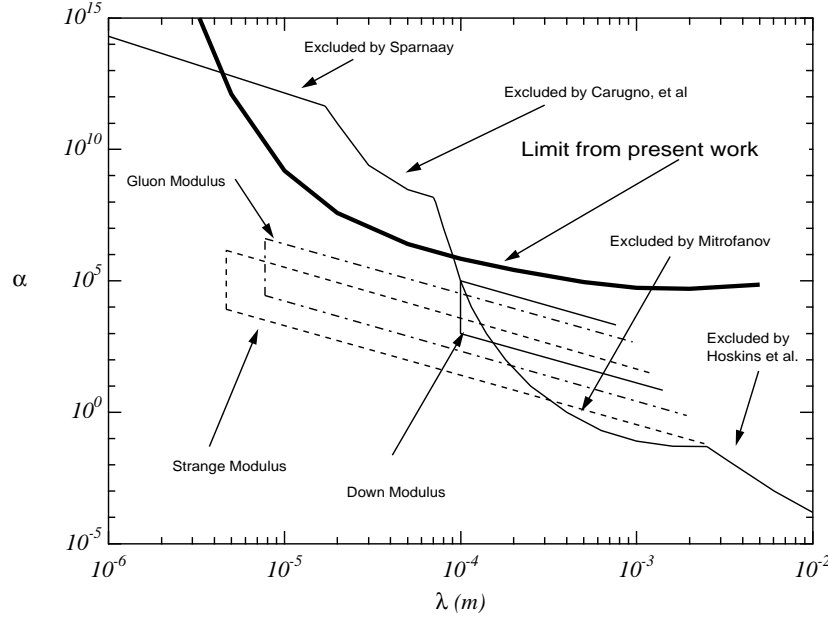


Figure 4: Anomalous force limit set by present work as compared with other experiments.

$d_0 = 0.2$ mm, a detection limit of $\alpha = 14$ could be expected, spanning the region of current theoretical interest. At this stage it is not clear whether this resolution is realistic, due to lack of any database on the required low frequency mechanical oscillators, and issues with vibration isolation. Our approach has been iterative, seeking to push down α as much as practical. Nevertheless, it seems reasonable to expect to reach $\alpha = 30 - 100$, perhaps operating in the range 3 - 10 Hz. This would allow a large fraction of the phase space occupied by the supersymmetry theories to be investigated. An improved apparatus designed to operate at low temperatures is under development.

ACKNOWLEDGMENTS

We wish to thank the NASA Office of Life and Microgravity Sciences and Applications for its support with grant # NAG8-1436.

REFERENCES

- 1: E. Fischbach et al., Phys. Rev. Lett., **56**, 3 (1986).
- 2: J.K. Hoskins et al., Phys. Rev. D, **32**, 3084 (1985).
- 3: M.J. Sparnaay, Physica, **24**, 751(1958).
- 4: G. Carugno, Z. Fontana, R. Onofrio and C. Rizzo, Phys. Rev. D, **55**, 6591 (1997).
- 5: V. P. Mitrofanov and O. I. Ponomareva, Sov. Phys. JETP, **67** (10), 1963 (1988).
- 6: J.N. Israelachvili and D. Tabor, Proc. Roy. Soc. Lond., A **331**, 19 (1972).
- 7: S. Dimopoulos and G.F. Giudice, Phys. Rev. Lett., **B379**, 105 (1996).
- 8: D.F. McGuigan et al., J. Low Temp. Phys., **30**, 621 (1978).
- 9: T.R. Albrecht, P. Grutter, D. Horne and D. Rugar, J. App. Phys., **69**, 668 (1991).
- 10: J.C. Price, Proc. Int. Symp. on Experimental Gravitational Physics, (ed: P.F. Michelson, Guangzhou, China, World Scientific, 1988).

TESTING RELATIVITY WITH CLOCKS ON SPACE STATION

J. A. Lipa, J. Nissen, S. Wang, D. Avaloff, S. Buchman, and J. P. Turneaure

W. W. Hansen Experimental Physics Laboratory, Stanford University, Stanford, CA 94305

With the approach of the Space Station era new interest has been kindled in performing fundamental physics experiments in space with time scales of months. Recently a microwave cavity clock experiment was selected for flight around 2007, to perform experiments in relativity. The project has four main goals: an improved test of Local Position Invariance, improved Kennedy-Thorndyke and Michelson-Morley type experiments, and an enhancement of the performance of atomic clocks being developed elsewhere for use in space. We describe the background and status of the project, which involves the development of a superconducting microwave oscillator with high frequency stability. On Space Station unwanted cavity frequency variations are expected to be caused mainly by acceleration effects due to residual drag and vibration, temperature variations, and fluctuations in the energy stored in the cavity. At present, acceleration effects appear to be the predominant limit, and a new cavity support system has been designed to reduce the effect. Fractional frequency stabilities in the low 10^{-16} range are expected on time scales of minutes.

INTRODUCTION

With the advent of laser-cooled atoms, the prospects for substantially more stable atomic clocks have dramatically improved. It now appears that laser-cooled cesium and rubidium frequency standards with stabilities of better than 10^{-16} are feasible in space, and single atom clocks with stabilities of 10^{-18} are discussed. When coupled with superconducting cavity oscillators (SCOs) these developments open up additional possibilities for experiments in fundamental physics. On large length scales and under extreme conditions Einstein's theory of general relativity encapsulates many of the fundamental physical laws used for predicting the intertwined behavior of matter and space. One of the most fundamental aspects of this theory is the behavior of clocks. So far, these have been used to test the theory in three different ways. A hydrogen maser was used¹ to measure the gravitational red shift to about a part in 10^4 using a rocket flight to an altitude of 10,000 km. The time delay for electromagnetic signals passing close to the sun has been measured² to a part in 10^3 . Finally, the assumption of Local Position Invariance (LPI) in the Einstein Equivalence Principle has been tested³ to 2%. Beyond general relativity, clocks have been used to test some of the foundations of special relativity by looking for effects due to a possible anisotropy of the velocity of light⁴, and to set bounds⁵ on the present rate of change of the fine structure constant.

To date, only atomic clocks have been used in space-based missions. Yet, for periods of up to about 1000 seconds, SCOs have provided the best frequency stability⁶. The major disadvantages in their application have been the degraded stability at longer times and the complexities of using cryogenic technology in space. In recent times the latter objection has become less compelling with the flight demonstrations of COBE and IRAS, both operating at low temperatures for about a year. Also, a recent shuttle flight has demonstrated on-orbit helium re-supply capability⁷. The Low Temperature Microgravity Physics Facility (LTMPF) planned for the International Space Station (ISS) will allow relatively cheap access to temperatures as low as 0.5 K in space for a wide range of missions with durations of up to a few months. A variety of atomic clocks are being developed for flight on the ISS, with very good stability for time periods in excess of 1,000 seconds. In collaboration with JPL, we are developing a superconducting

microwave oscillator (SUMO) which should significantly augment the scope and capability of the space clock ensemble. SUMO is essentially a space version of the SCO. Comparing the resonant frequencies of three niobium cavities operating near 8.6 GHz, a fractional frequency stability of $\sim 3 \times 10^{-16}$ was achieved⁶, and unloaded quality factors as high as 10^{11} were observed. For comparison, recent work with superconductor-coated sapphire resonators⁸ and compensated sapphire oscillators⁹ have reached short-term frequency stabilities between 10^{-14} and 10^{-15} .

The LPI principle of general relativity states that clocks made in different ways all keep exactly the same time, no matter where they are co-located in the universe. This might not be true if some of the laws of physics vary slightly from place to place. One of SUMO's science goals is to perform an improved LPI test by comparing the microwave cavity frequency with that of an atomic clock to a part in 10^{16} , as a function of position and gravitational potential. The gravitational potential varies with the orbital motion of the ISS, as well as with the Earth's motion in its eccentric orbit around the Sun. A basis of the test is the observation that the frequencies of a microwave cavity and an atomic clock have different dependencies on fundamental physical constants³. Alternatively, one can view the experiment as setting limits on effects predicted by various theories competing with general relativity as descriptions of the interaction of matter and space. This test is expected to improve the earlier measurement by a factor of about 100.

Tests of the foundations of special relativity fall into two main classes: one involving angle-dependent effects and the other absolute velocity effects. A generalized treatment of the Lorentz transformations has been given by Mansouri and Sexl¹⁰ who consider the possibility of an anisotropic propagation velocity of light relative to a preferred frame. If a laboratory is assumed to be moving at a velocity v at an angle θ relative to the axis of a preferred frame, the speed of light as a function of θ is given by

$$c(\theta)/c = 1 + (1/2 - \beta + \delta)v^2/c^2 \sin^2\theta + (\beta - \epsilon - 1)v^2/c^2 \quad (1)$$

where ϵ is the time dilation parameter, β is the Lorentz contraction parameter, and δ tests for transverse contraction, to be determined either experimentally or in the particular theory being considered. In general relativity the last two terms on the right hand side of equation 1 are zero. In a Michelson-Morley experiment the amplitude of the θ -dependent term is measured, while in a Kennedy-Thorndyke experiment the amplitude of the θ -independent term is determined. To evaluate experiments it is often assumed that the preferred frame is the rest frame of the cosmic microwave background. In this case by far the biggest contributor to v is the apparent velocity of the earth along the anisotropy axis, approximately 370 km/sec. For an experiment on Space Station, the relative velocity would be modulated at orbital rate as measured in inertial coordinates, giving rise to the periodically varying clock signal. It is generally assumed that the frequency of a laser-cooled atomic clock is independent of the velocity vector.

Since the modulation of v is due to the Space Station orbital motion, it is clear that certain flight times could be more favorable than others to perform the experiment. Also, since the orbit plane precesses at approximately $5^\circ/\text{day}$, significant changes in the signal would be expected with time. This easily modeled signature would be valuable if an effect was detected. However, the potential variability argues for the longest possible mission, to provide the greatest angular changes in the velocity vector of the clocks. In the case of the θ -dependent class, a signal could be generated by mounting two cavities at right angles, since their frequencies are sensitive to the velocity of light only in the radial directions.

Presently the best limit¹¹ on this form of isotropy is $\Delta c/c < 2 \times 10^{-13}$. By comparing the frequencies of two orthogonally mounted cavities at twice orbital roll rate, the expected limit for this effect could be reduced to $\Delta c/c \sim 10^{-16}$. The present limit¹¹ on the KT term is $(\beta - \epsilon - 1) < 6.6 \times 10^{-5}$. With an Allan variance of 5×10^{-16} referencing to an atomic clock, and averaging over 100 orbits, we would expect to set a limit of $\sim 8 \times 10^{-10}$, a factor of 8×10^4 improvement. This signal would be modulated at orbital rate.

For intervals in the range 1 - 100 sec. SUMO can provide a high stability, low phase noise signal capable of being slaved to atomic clocks, providing them with a 'flywheel' and greatly enhancing their performance. SUMO will be an insert in the LTMPF and will require three to six months of operation in order to meet its science objectives. Longer-term experiments, using two or more oscillators and separate facilities, include precision red-shift measurements and possibly the detection of gravitational waves. The possibility of using SCOs for pulsar timing in space has also been mentioned¹².

APPARATUS

The apparatus for testing the stability of cavity oscillators is based on a three-cavity setup built for the earlier LPI experiment³. The microwave resonators are formed from highly annealed niobium and operate in ultrahigh vacuum at about 1.3 K. Mechanical stability is achieved by making the walls of the cavity about the same thickness as its 1.3 cm radius. The cavities are supported from the top and connected with indium-sealed vacuum flanges to pump-out ports and waveguides. High vacuum conditions for the cavities are maintained by means of a permanent internal vacuum with a pinch-off seal. A Cryoperm magnetic shield is used to reduce the field at the cavity to $\sim 10^{-3}$ Gauss. The connections between the cavities and the room temperature electronics are made using stainless steel waveguides with copper baffles in order to minimize the heat input to the cryogenic environment.

The SCO electronics system utilizes the high Q cavity resonance to stabilize a voltage-controlled oscillator (VCO). A small part of the power of the VCO is used to excite the cavity. This signal is phase-modulated at 1 MHz, and the amplitude-modulated component reflected by the cavity is detected. The sign and amplitude of this signal represent the deviation of the VCO frequency from the cavity frequency, and are used to servo the VCO frequency. Figure 1 shows a block diagram of a frequency control loop. The present VCO is a varactor-tuned dielectric resonator oscillator. The outputs from up to three VCOs locked to individual cavities are beat against each other to produce difference frequencies of a few tens of Hz, which constitute the ensemble output. These signals are processed digitally to provide Allan variance information as a function of sampling time.

RECENT PROGRESS

The unloaded quality factors of the original cavities were re-measured to be in the range of 1.6 to 3.7×10^{10} at 1.5 K after long term storage in vacuum. Tests were also conducted to evaluate their stability. Figure 2 shows the Allan variance of frequency differences for two cavities during an 8-hour period using a new electronics system. The noise floor appears to be in the range of 3 to 6×10^{-16} for measuring times > 100 seconds. To date, no vibration or tilt compensation has been implemented, and the temperature has

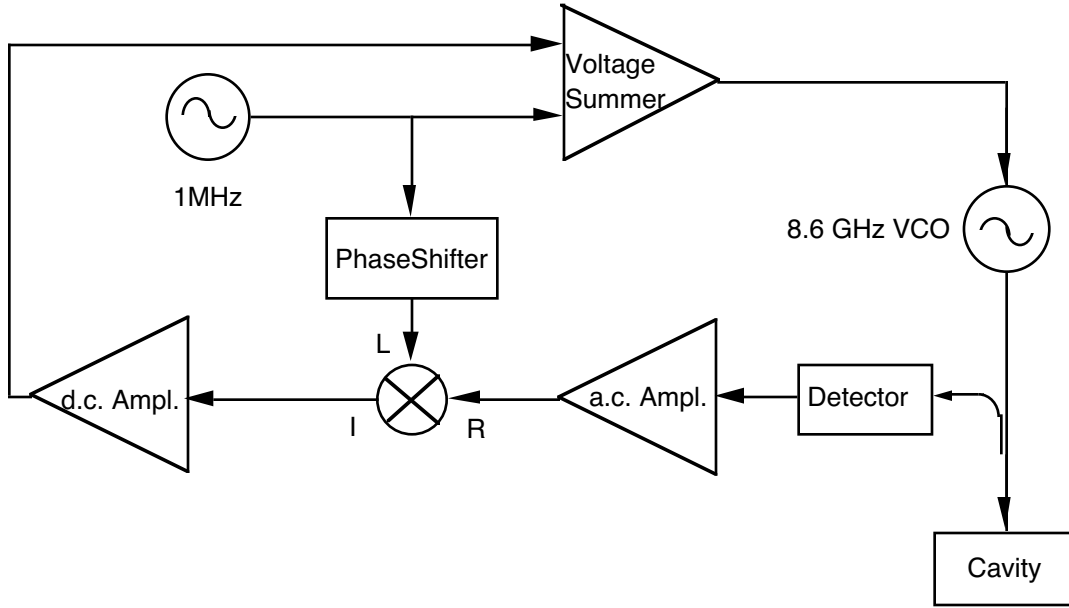


Fig. 1: Block diagram of the oscillator frequency control loop.

been controlled to only about 5 μK , at an operating temperature of 1.3 K. The primary limitation on the frequency stability for this setup appears to be small variations in tilt. Since the cavities are end-mounted, there is a small variation of the radius with tilt due to the Poisson ratio. Correlations between tilt and frequency have been demonstrated. A secondary cause of instability is due to changes in the profile of the temperature along the waveguides linking the cavities to the DROs at room temperature. To reduce this effect we are developing a new setup in which the directional coupler and the detector are located at low temperatures, and the waveguides are replaced with coaxial cables with selected attenuation. Initial tests with this configuration have been favorable.

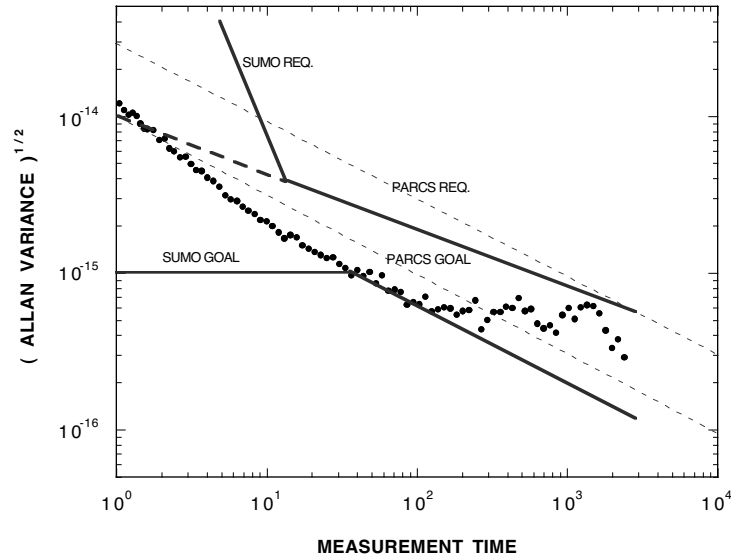


Fig. 2: The Allan variance of frequency differences of two cavities at 1.3K, as a function of measurement interval.

CAVITY DESIGN

Accelerations of the cavity, such as that due to the earth's gravitational pull, cause distortions in its shape. When these distortions are perpendicular to the cavity walls, they can cause a shift in the cavity resonant frequency. To minimize the frequency changes that occur due to changing accelerations we have designed a new supporting structure for the cavity that takes advantage of some of the symmetries in the cavity design. The new design is based on a finite-element analysis of the effects of acceleration on the cavity dimensions, and numerical calculations of the fields inside the cavity at the walls, plus the perturbation of the energy of the fields in the cavity due to the wall displacement. Supporting the cavity radially around its center reduces the sensitivity of the frequency to acceleration because of symmetry. With an end-support the calculated frequency change is about $6.5 \times 10^{-9} \Delta f/f$ per g, while with an ideal center support this number falls to below 10^{-17} . Allowing for machining errors, a realistic center support gives numbers closer to 10^{-12} . By varying the geometry of the supporting structure one could theoretically reduce the frequency shift to zero, but this would require precise control of cavity and support dimensions as well as a high confidence in the numeric calculation. Some tuning may be done during testing.

Calculations for the cases of the gravity vector perpendicular to the axis of symmetry had to be performed in three dimensions. When the gravity vector is off axis, the overall displacement of the cavity is much greater than the non-symmetric distortions we are sensitive to. Because of this, numeric noise in the three dimensional calculations was clearly visible at the level of $10^{-13} \Delta f/f$ per g. There were no asymmetric distortions of the cavity above this noise floor when the gravity vector was perpendicular to the cavity axis. Figure 3 shows a cross-sectional view of the new cavity now in test.

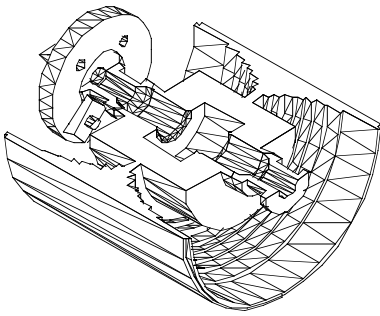


Fig. 3: Cut-away view of the acceleration-compensated cavity design.

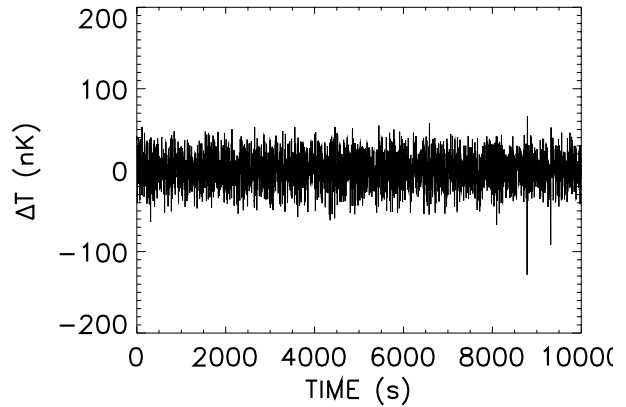


Fig. 4: Temperature stability as a function of time as seen on the CHEX Shuttle mission, using high resolution thermometry techniques.

TEMPERAURE STABILIZATION

Near 1.3K the temperature coefficient of the cavity frequency is typically $\Delta f/f \sim 3 \times 10^{-10}$ per degree. Thus to achieve a signal resolution of 10^{-16} at orbital periods we need to control the cavity temperature to about $\pm 3 \times 10^{-7}$ K. The recent flight of the CHEX experiment¹³ on the Shuttle has demonstrated that this is within the range of existing capability using advanced high resolution thermometry techniques. In Figure 4 we show some of the data from a temperature controller used in that experiment during a period when the instrument was held at constant temperature. The thermometry used was a specially developed paramagnetic salt detector with a superconducting magnetometer readout system. It can be seen that the rms. stability is below 3×10^{-8} K, much better than our needs. It can also be seen that most of the noise is short term, while for 45 and 90 minute periods the control level is even better. Other measurements indicate that the absolute drift of temperature with time can easily be held below 10^{-13} K/s, which is negligible in the present application. We plan to use a modified version of this thermometry technique to control the temperature of the cavity, minimizing temperature-induced frequency variations. Previous thermometers¹⁴ used a copper ammonium bromide salt as the paramagnetic sensor. Since our operating temperature is well below the Curie temperature of this salt, we have had to develop a new type of sensor¹⁵. Our current sensor is a rod of a palladium-manganese alloy with 99.59 atomic percentage Pd and 0.41% Mn. This should have¹⁶ a Curie temperature of about 1K. The transition temperature of this alloy can be adjusted to any desired temperature below 4K by changing the concentration of Mn. Besides the tunability of the transition temperature, this alloy is easier to work with than the paramagnetic salts. However, we are carrying the salt Manganous Ammonium Sulfate as a backup. This material has a very low Curie point and a high sensitivity to temperature over a wide range.

The major issue with thermal control is the varying energy dump from charged particle radiation as the experiment moves around the ISS orbit. We can make an estimate of this effect by scaling from the observations on CHEX to the present situation. It is expected that the variations in the radiation environment will be as much as a factor of five worse on ISS relative to the 28° inclination Shuttle case, but since the 45 min cycle is not visible in Figure 4, we expect to have adequate margin relative to the $\pm 3 \times 10^{-7}$ K requirement. A more quantitative analysis is in progress.

CONCLUSIONS

We have described a project to place superconducting cavity oscillators in orbit on Space Station. The original cavity oscillator technology demonstrated a frequency stability approaching 3×10^{-16} for time intervals between 30 and 1000 seconds. Our recent measurements have achieved levels of $\sim 5 \times 10^{-16}$ for time scales of 100 to 3000 seconds at 1.3 K, competitive with modern atomic clocks. A design suitable for use in space is under development. On the Space Station, the cavities can be used in conjunction with atomic clocks to perform tests of relativity, and as low phase-noise flywheels for atomic fountain experiments. Our analysis of the limitations of superconducting cavity oscillators indicates that improvements to the 10^{-17} range are quite possible.

ACKNOWLEDGMENTS

We wish to thank the NASA Office of Life and Microgravity Sciences and Applications for its support with grants # NAG3-1940 and NAG8-1439, W. Moeur and M. Dong for substantial assistance in the initial phases of the project, and J. Mester for help with magnetic susceptibility measurements.

REFERENCES

1. Vessot, R.F.C., et al., *Phys. Rev. Letts.* **45**, 2081 (1980).
2. Shapiro, I., *Phys. Rev. Letts* **13**, 789 (1964).
3. Turneure, J.P., Will, C.M., Farrel, B.F., Mattison, E.M., and Vessot, R.F.C., *Phys. Rev. D* **27**, 1705 (1983).
4. Will, C.M., *Phys. Rev. D*, **45** 403 (1992).
5. Prestage, J.D., Tjoelker, R.L., and Maleki, L, *Phys. Rev. Letts.* **74**, 3511 (1995).
6. Stein, S.R., and Turneure, J.P., *Proceedings of the IEEE*, 1249 (1975).
7. DiPirro, M. J., Shirron, P. J., and Tuttle, J. G., *Cryogenics* **34**, 267 (1994).
8. Luiten, A.N., Mann, A.G., and Blair, D.G., *Electronics Letts.* **30**, 417 (1994).
9. Dick, G.J., Wang, R.T., and Tjoelker, R.L., *Proc. IEEE Int. Freq. Control Symposium*, **98CH36165**, 528 (1998).
10. Mansouri, R. and Sexl, R.U., *Gen. Rel. and Grav.* **8**, 497 (1977).
11. Hils, D., and Hall, J.L., *Phys. Rev. Letts.* **64**, 1697 (1990).
12. Strayer, D., and Yeh, N-C., private communication (1998).
13. Lipa, J.A., Swanson, D.R., Nissen, J.A., Geng, Z.K., Williamson, P.R., Stricker, D.R., Chui, T.C.P., Israelsson, U.E., and Larson, M., *Phys. Rev. Letts.* **84**, 4894 (2000).
14. Lipa, J.A., Swanson, D.R., Nissen, J.A., and Chui, T.C.P., *Cryogenics* **34**, 341 (1994).
15. Klemme, B.J., et.al., *J. Low Temp. Phys.* **116**, 133 (1999).
16. Nieuwenhuys, G. J., *Adv. Phys.* **24**, 515 (1975).

